Dear Dr. Nunzio Romano,

We would like to thank you and three reviewers for the insightful comments and evaluation of this manuscript. We have carefully revised the manuscript and have addressed all reviewers' comments one-by-one accordingly. Specifically, we have addressed three major revisions to the manuscript as follows: (1) We have thoroughly improved the quality of figures in the manuscript. For instance, we have added the wind rose to Figure 1. Figure 4 on the model implementation has been added to illustrate the workflow of this study. We have changed the Figure 7 to boxplots. We have merged the daily, half-hourly and monthly validation results to Figure 8. (2) We have also improved the descriptions on the model implementation, structure and parameter abbreviation, and eddy covariance flux data processing. (3) We have added discussion on future improvement for the SVEN model and the potential challenges for the implementation of our approach with satellite Earth observation to the large scale.

Our responses to all reviewers' comments are in the section below. The original reviewer comments are in black and our responses are in red.

Thanks for your assistance!

Sincerely yours,

Sheng Wang

Reviewer 1:

Response to the review of Referee 1. We have copied the comments of the referee hereunder with our comments appearing after the referee's comments.

This study "Temporal interpolation of land surface fluxes derived from remote sensing results with an Unmanned Aerial System" developed a simple but operational land surface modeling framework, simulating energy balance, water and CO2 fluxes between the land surface and the. Unmanned aerial system (UAS) can be applied flexibly, and can have high spatial-temporal resolution data, which is used widely in recent decades. This study used UAS to provide optical and thermal data as model inputs for land surface-atmosphere fluxes monitoring. A dynamic soil vegetation atmosphere transfer model was developed here, together with the PT-JPL ET model and light use efficiency GPP model for simulating energy, water and CO2 cycles. The results showed that with using the data from UAS optical and thermal observations, the models were capable to simulate the energy, water and CO2 fluxes in a deciduous tree plantation area, indicating that the UAS observations could be served as "ground truth" to calibrate soil and vegetation parameters, highlighting the usage of multiple remote sensing data for land-atmosphere flux monitoring. I think this manuscript is well written and the logic is pretty clear. The results are supported by the data shown here, while the authors explained the results adequately and clearly, though I have several minor questions on the current manuscript.

Reply: Thank you for the insightful comments and suggestions, which are very helpful to improve the manuscript. We totally agree that the great potential of utilizing UAS for monitoring land surface energy, water and CO_2 processes. The proposed model in our study is capable of temporal interpolating the remote sensing based snapshot estimates into the continuous records. Here, we have addressed your comments point-by-point.

(1) Introduction, why not introduce more about UAS? This is kind of a highlight of this study to use UAS data. Maybe include some introductions about recent studies using UAS data on GPP/ET simulations?

Reply: Thank you for the comments and suggestions. We have revised the introduction to add more review contents about UAS, particularly on applying UAS data for GPP / ET estimation. Please see Line 13-20 on P2 in the revised clean version.

(2) Why there is no UAS observation in July, and between May 25th and June 24th? In Fig. 2(c), the fIPAR seems to change a lot during 25/May to 24/June, thus, no observation during this time period may induce simulation errors in the model.

Reply: Thank you for the comments and suggestions. We totally agree with the reviewer's opinion on the importance of collecting observations during the period from May 25th to June 24th. However, due to technical issues, we did not manage to fly UAS over that period. On the other side, this low frequency of collecting UAS observations provides an opportunity to demonstrate that the "ground truth" collected from sparse remote sensing observations can be utilized to be temporally interpolated to obtain the continuous estimates.

(3) Why ignore the observation on 24/June when interpolate the UAS data.

Reply: Thank you for the comments and suggestions. We do incorporate the observation on June 24th into the temporal interpolation, but the observation on June 24th is not from UAS. The observations on that day are from the ground PAR sensors (Table 1). Due to technical issues, we did not manage to fly UAS over that period. However, to demonstrate the potential to use the proposed SVEN model to temporally interpolate the snapshot estimates, we have incorporated the ground IPAR observations on June 24th to simulate the process of vegetation growth in this period. To make the context clearer, we have revised the sentence on L10-15 on P6.

(4) Page 16, Ln. 2-3, not fully understand "This demonstrates that SVEN is capable to : : :.", syntax error?

Reply: Thank you for the comments and suggestions. We have revised this sentence. It should be that "Such simulation accuracy demonstrates that SVEN is capable of temporal interpolating the snapshot estimates or observations between remote sensing acquisitions to form continuous daily records." Please see L11-13 on P17.

(5) Fig. 5(a), Ts, kind of systematic overestimation of Ts sim compared to Ts obs? So can the model parameters be calibrated to reduce the overestimation?

Reply: Thank you for the comments and suggestions. Yes, we can try to reduce the systematic overestimation of Ts through calibration. However, this study used multi-objective calibration procedures to consider both Ts and soil moisture. As results shown in the Pareto Front of Figure 5, if we want to obtain better performance of simulating Ts, the performance of simulating soil moisture could be degraded. Thus, based on the Pareto front in Figure 4, we choose the parameter sets to achieve relatively good simulations for both Ts and soil moisture. To make this context clearer, we have revised the manuscript. Please find the revised sentences of L20-25 on P16.

(6) Fig 5(c), the scatterplot of SM sim and SM obs is kind of wired, which is more obvious in Fig. 7, I am wondering why? And also why not show daily results together with the half-hourly and monthly results in Fig. 7.

Reply: Thank you for the comments and suggestions. They are very helpful. There are several reasons for the moderate performance of simulating soil moisture in this study. Such model performance may be due to the uncertainty in the model parameters related to θ. As shown in supplemental Table S5, the effective parameter values of the infiltration rate for the saturated soil (Ks) and fitting parameter of the Mualem model (n) were taken as the mean values from the look-up table without considering ranges of variability (standard deviations in the table). In fact, only one parameter, SWS_{max}, among the three parameters related to θ dynamics was calibrated with UAS estimates of θ in the root zone. To keep the model simple and operational, the SVEN model only used one soil layer to simulate the dynamics of soil water storage (Figure 3). Such simplification could also contribute to the relatively moderate performance of simulating θ. Additionally, UAS derived θ estimates used for calibration have errors of around 13% (Wang et al., 2018a), which can induce uncertainties in the simulated time series through error propagates in the parameter calibration. Furthermore, only seven snapshot estimates from UAS were used to calibrate the model with an average frequency of 25 days during the period of fast growth. It can be expected that

improving the UAS based estimates of θ and increasing the number of observations for model calibration can improve the simulation performance. To elaborate details on the simulation performance of soil moisture, we have added discussion in L3-13 on P19.

Thank you for the suggestion on the figure. We agree that combining daily results together with the half-hourly and monthly results could be better. We have revised Figure 7 and combined it with Figure 5 according to the reviewer's suggestions.

Reviewer 2:

Response to the review of Referee 2. We have copied the comments of the referee hereunder with our comments appearing after the referee's comments.

This manuscript introduces a simple but effective coupled surface exchange model, with the goal to use it for gap filling of surface states and fluxes between measurements by remote sensing. The model requires higher resolution meteorological data as input for the forward simulation that serves as the gap filling procedure. The calibration is based on a very small number of snap shots of surface temperature and Normalized Difference Vegetation Index. As a proof of concept the method is applied using data obtained during seven flights of a drone, and continuous data from an eddy tower. The performance of the model es evaluated by comparing with independent eddy tower data of fluxes and states.

The manuscript presents an intriguing approach tested in a well designed study. The results are impressive, especially given the deliberate simplicity of the applied exchange model. The manuscript is well written manuscript. While I have some comments on the manuscript, I also recommend its publication in HESS and expect that it will find strong interest in the readership.

Reply: We appreciate the reviewer's insightful comments and suggestions, which were very helpful to improve the manuscript. We totally agree that the great potential of utilizing the simple but effective land surface models to fill gaps between observed surface states and fluxes from remote sensing. Here, we have addressed your comments point-by-point.

Major comments

(1) I found if very difficult to disentangle the different data sources used for the different application steps, which are: parameter estimation from literature and nearby observations calibration (UAS derived data, surface temperature and soil moisture) input for forward modeling (meteorological data from the eddy tower) validation of model output (independent eddy tower data) To make this more accessible I am missing an overview table systematically showing which data source was used for what purpose (as above). This would really help navigation,

Reply: Thank you for your suggestions. To make the data and parameter sources clear, we have added one figure on the flow chart of this study. Please see Figure 4, which includes details on the model inputs, parameter, outputs and calibration procedures. We also have added the sources of parameter values into the figure. For details, please refer to L1-5 on P14 in the revised clean version.

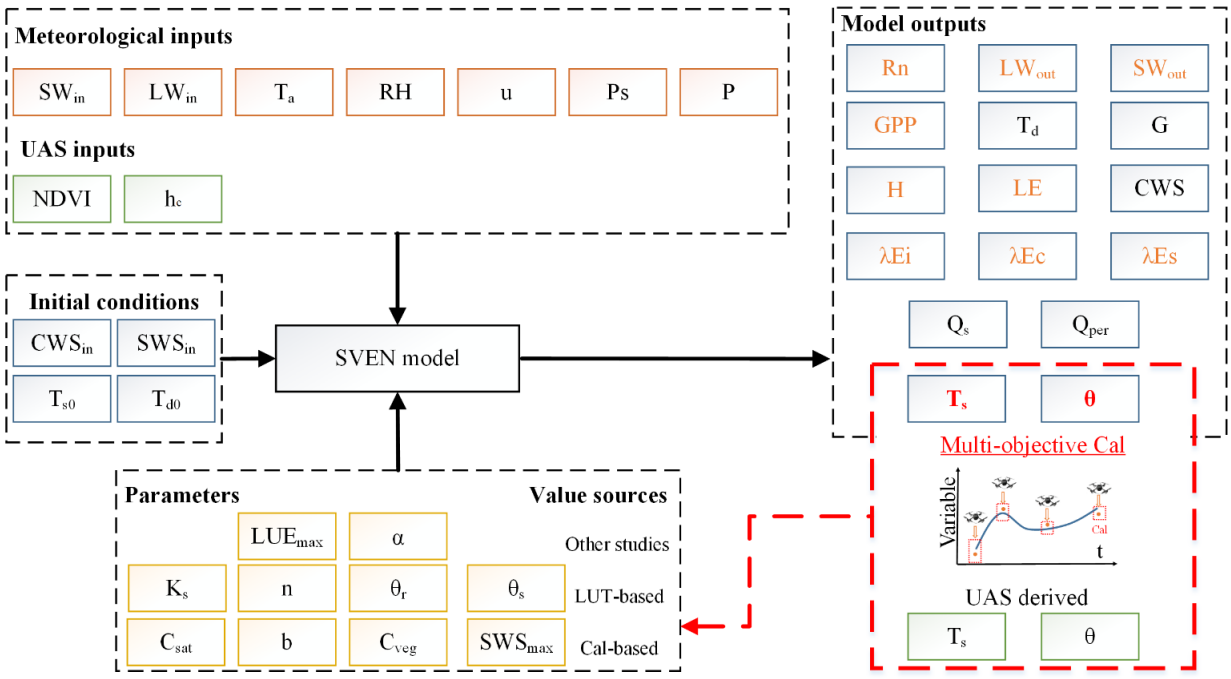

Figure 4. Model implementation of this study. UAS and meteorological data were used as inputs of the SVEN model. Values of the SVEN parameters were obtained from the look-up table, other studies, or model calibration with UAS derived variables. In the model outputs, variables with the highlighted red colour (T_s and θ) refers to the variables calibrated with UAS derived observations or estimates. The variables with orange colours are retrievable from remote sensing techniques. For abbreviations, please refer to the list of abbreviations for model variables and parameters in the supplementary.

(2) I would have liked to see some more discussion on the next challenges for the more widespread application of the proposed method with less ideal input data for the forward model. What are the expected limitations of the approach? Currently the discussion regarding this point is very short. For example, the discussion mentions that the method could be extended to larger scales by using online weather data. However, those have also higher uncertainty compared to the data from the tower. Also, the JPL-Priestley-Taylor-ET estimate is less reliable in more arid climates which probably requires additional adjustments in those conditions, etc. I recommend enhancing the discussion regarding this.

Reply: Thank you for your suggestions. We agree that there are still challenges and limitations for the more widespread application of the proposed model, particularly when applying models to the large scales and data-scarcity regions. First of all, the SVEN model is a very simple and parsimonious process-based model. For instance, the current soil moisture module in the SVEN model is a simple water balance model with considering one soil layer, which has limited capacity to simulate soil water dynamics particularly in regions with complex landforms. In addition, the soil layer depth refers to the maximum root water uptake depth, which can vary with time, but SVEN simplified this soil depth parameter to keep it consistent. Thus, in our study, SVEN only achieved moderate performance to simulate soil water dynamics and it can be expected that in water limited drylands, soil moisture simulation has a larger impact on the ET than in our site. Additionally, compared to the Penman-Monteith approach, the Priestley–Taylor approach may need adjustment of the aerodynamic term, when extending the study from radiation controlled sites to arid climates. Regarding the model-data integration, our study used a two-

objective optimization scheme, there are more advanced algorithms e.g. data assimilation could enable the consideration of data and model uncertainties in the integration process.

Moreover, when applying the model with satellite coarse resolution data to the large scale, there will be four major impacts. First, the space-borne remote sensing data have much coarser spatial resolution. If we move the simulation to the large scale with satellite data, we need to find accurate gridded meteorological data as forcing. UAS imagery has limited coverage and thus this study only used one meteorological station data as forcing.

As satellite data have coarser pixel sizes, we also need to consider the sub-grid heterogeneity and identify the effective values for model parameters. Note all parameter values of models were obtained from parameter calibration with remote sensing based estimates. For instance, in our study, we used the look-up tables with soil texture information to identify soil parameter values. In the large-scale simulation with satellite data, the plant functional type and soil type parameterization scheme for different ecosystems and environmental conditions would be needed. However, the integration of accurate remote sensing estimates with land surface models would be beneficial to reduce the dependency of plant functional type parameterization schemes and achieve a higher accuracy to predict land surface variables.

In addition, coarse resolution satellite data may have limited accuracy to predict land surface fluxes compared to the detailed UAS data. Applying SVEN with satellite data to large scale, we also need to be careful about the accuracy of remote sensing based estimates and the error propagation from the model inputs to the outputs.

Satellite data in the optical and thermal ranges can only provide observations during the sunny weather conditions. However, the UAS data in this study were collected in both sunny and cloudy conditions. We envision that using satellite based data to calibrate model may lead the model estimates biased towards the sunny conditions.

We also agree with the reviewer that compared to the Penman-Monteith approach, the Priestley–Taylor approach may need adjustment of the aerodynamic term, when extending the study from radiation controlled sites to arid climates.

We have added these contents regarding the model improvement and challenges to the discussion part. For details, please refer to section 4.4 in the revised clean version.

(3) I am confused about what is the underlying hypothesis motivating the comparison of the residuals across different stages of diffuse light conditions? The analysis is motivated by stating that remote sensing is typically biased towards collection in direct sunlight conditions. But this was probably not the case in your exercise, since you were collecting data from a drone. Therefore the calibration data set should not be affected by this bias? Why are you expecting the bias in the residuals?

Reply: Thank you for your comments. We have revised Figure 7 to be boxplots to make the results clear. We agree that due to that UAS data collection happens on both sunny and cloudy weather conditions, we did not see significant differences of residuals in simulating surface temperature, net radiation, soil moisture, latent heat flux, and gross primary production for different sky conditions. We have revised the description and for details, please refer to L6-10 on P20.

(4) I find the equations of the manuscript difficult to read because the abbreviations of the variables are of several letters. I understand that in some instances this is done to adhere by the nomenclature in the discipline, e.g converting LAI to a one letter variable would probably cause confusion. But in most cases this is not an issue. For example, radiation can be abbreviated with R and the components by indices, fluxes with Q or J with indices. Also canopy storage, soil water storage etc. This would also increase consistency. I strongly recommend incorporating the one letter abbreviation paradigm as much as possible. See also HESS author guidelines (Mathematical requirements) https://www.hydrology-and-earth-systemsciences.net/for_authors/manuscript_preparation.html

Reply: Thank you for your suggestions. We have revised the abbreviations of variables to be one letter abbreviation as much as possible. For instance, we used ALB to represent surface albedo in the previous version. In the revised version, we used one letter abbreviation A to stand for surface albedo. Please see L15 on P8. (Notably, most studies used the Greek letter α to represent surface albedo. However, α has already been used as the PT coefficient in Eq. 22.) We also have changed soil moisture (SM) to one Greek letter θ. We have changed the wind speed from WS to u. Furthermore, we have also summarized all abbreviations in the supplementary material.

Detailed comments

Abstract, Page 1

Line 18: "SVEN interpolated the snapshot Ts, Rn, SM, ET and GPP to continuous records“ This phrase is confusing, as it sounds like measurements of each of those variables were used, when according to the methods section only Ts and NDVI were used for calibration.

Reply: Thank you for your suggestions. We have revised this sentence to be clearer. Based on model parameter calibration with the snapshots of land surface variables at the time of flight, SVEN interpolated the UAS based snapshots to continuous records of T_s, Rn, θ, ET and GPP for the growing season of 2016 with forcing from continuous climatic data and NDVI. Please see L17-19 on P1.

Line 21-22 I would not mind, if the errors were not stated quantitatively here, but if this is desired: An indication of the errors in percent would be more meaningful.

Reply: Thank you for your suggestions. In order to make clearer, we have added the statistics to be in percent (normalized root-mean squares deviations, NRMSD). The NRMSD was calculated as the ratio between root-mean squares deviations and the range (maximum minus minimum) of observations. Please see L20-21 on P1.

Introduction

Line 19/20: I think you mean "high persistence“

Reply: Thank you for your suggestions. It is a mistake. We have changed the word to “high persistence”. Please see L25 on P2.

Methods

Page 9, Line 5 "low pass filter for T_s“: Can you be more specific about the cutoff frequency? Which interval does this roughly refer to?

Reply: Thank you for your suggestions. The cutoff frequency is 24 hours. We have revised the sentence in L21 on P9. T_d refers to the deep soil temperature (°C) calculated by applying a low-pass filter to T_s with the cut-off frequency of 24 hours.

Page 9 Line 24 Wind speed seems to be one of the variables that need to be available continuously to apply the method. Is it reasonable to have such good knowledge of the wind speed? How sensitive is it?

Reply: Thank you for your suggestion. Yes, the model needs the wind speed as inputs to calculate the aerodynamic resistance for estimating sensible heat fluxes. The accurate information about the wind speed is important for the model to estimate the aerodynamic resistance to the transfer of sensible heat flux. Wind speed, however, it is not used to estimate the transfer of vapor flux (evapotranspiration) as we used a Priestley-Taylor JPL equation. The PT-JPL model used the PT coefficient (α) with a fixed value to account for the ratio between aerodynamic term and radiation. Thus, the ET is not sensitive to wind speed in the model. The larger contribution to errors in H is actually from the soil, canopy, and air temperature (Chehbouni et al., 2001). After that, uncertainties in soil and canopy emissivity values, canopy height, and wind speed also have measurable effects on the accuracy of simulating H (Sánchez et al., 2008). In addition, the error in the sonic anemometer is very low. With traditional cup anemometers, a larger error, of about 10% of error in the wind speed will translate in an error in H of about 5-10% (depending on the temperature difference) for the type of vegetation in this paper. In SVEN the surface temperature estimates depend on the energy forcing which is constrained by three different energy variables (Rn, H, LE) and soil moisture, apart from the temperature from the previous time step. Therefore, errors in wind speed only affect H should not affect too much the temperature estimates. However, we also agree that without field measurements such as the sonic anemometer, the wind speed data could have large uncertainties from weather forecasting or climate reanalysis data. Applying the SVEN model to the large scale or other data-scarcity regions could have more uncertainties from wind speed data. Thus, we have added these discussions about the uncertainties from wind speed to model performance. Please see L28-29 on P23.

Chehbouni, A., Nouvellon, Y., Lhomme, J. P., Watts, C., Boulet, G., Kerr, Y. H., ... & Goodrich, D. C. (2001). Estimation of surface sensible heat flux using dual angle observations of radiative surface temperature. *Agricultural and Forest Meteorology*, *108*(1), 55-65.

Sánchez, J. M., Kustas, W. P., Caselles, V., & Anderson, M. C. (2008). Modelling surface energy fluxes over maize using a two-source patch model and radiometric soil and canopy temperature observations. *Remote sensing of Environment*, *112*(3), 1130-1143.

Page 10, Line 15-20 The PF-JPL works much better in temperate then drier climate. Your appraisal does not mention this limitation, but I think it may be important for applying this method more generally. Could you add a note on this, either here or in the discussion?

Reply: Thank you for your suggestion. We agree that PT-JPL works better in temperate than drier climate. We also agree that it is good to mention the limitation of this model. We have added this suggestion to L24-26 on P23. Compared to the Penman-Monteith approach, the Priestley–Taylor approach may need adjustment of the aerodynamic term, when extending the study from radiation controlled sites to arid climates (Tadesse et al., 2018; Xiaoying and Erda, 2005).

Tadesse, H. K., Moriasi, D. N., Gowda, P. H., Marek, G., Steiner, J. L., Brauer, D., Talebizadeh, M., Nelson, A. and Starks, P.: Evaluating evapotranspiration estimation methods in APEX model for dryland cropping systems in a semi-arid region, Agric. Water Manag., doi:10.1016/j.agwat.2018.04.007, 2018.

Xiaoying, L. and Erda, L.: Performance of the Priestley-Taylor equation in the semiarid climate of North China, Agric. Water Manag., doi:10.1016/j.agwat.2004.07.007, 2005.

Page 11, Line 27 should probably be "equation 29“ instead of "equation 28“

Reply: Thank you for your suggestion. We have revised it.

Page 12 Line 2 Soil water storage has different units here (m) and on page 9, Line 10 (m^3). I think it is fine to stick with m.

Reply: Thank you for your suggestion. We have revised all units for soil and canopy water storage to be m.

Page 12, Eq. 30-32, Page 13 Line 19-20 I am not sure how theta_r and theta_s are dealt with? They are not calibrated and not mentioned for the look-up table. Based on Table S5, where they are included, I am assuming they were looked up too. But please be more specific and include them in the list of parameters in Table 2.

Reply: Thank you for your suggestion. theta_r and theta_s are from the look-up tables based on soil texture. I have revised Table 2 to include theta_r and theta_s. For details, please refer to Table 2 and Figure 4.

Page 13 Table 2 It will help navigating the text, if in the table included a column indication of whether this parameter was looked up or calibrated in this study. I suggest adding this.

Reply: Thank you for your suggestion. We have revised Table 2 and added one column to indicate the source of parameter values (model calibration or look-up table). Furthermore, we have added Figure 4 to show the model implementation of this study.

Page 13 Line 22 In my understanding calibrating SWS_max boils down to calibration the root water uptake depth?If yes, would be good to indicate this. While I have no objections against this procedure here, I conjecture that root water uptake depth may vary with time over the growing season. Thus, this may be a limitation of the model, which could be mentioned in the discussion.

Reply: Thank you for your suggestion. We agree that the root water uptake depth vary with time over the growing season. Our paper aims to propose a simple but operational model for interpolation of land surface states/fluxes. So we did not consider such variations of root water uptake depth. To address this limitation, we have added discussion on the shortage of this model into the discussion part. Please find L18-19 on P23. In addition, the soil layer depth refers to the maximum root water uptake depth, which can vary with time (Guderle and Hildebrandt, 2015), but SVEN simplified this soil depth parameter to keep it consistent.

Guderle, M. and Hildebrandt, A.: Using measured soil water contents to estimate evapotranspiration and root water uptake profiles-a comparative study, Hydrol. Earth Syst. Sci., doi:10.5194/hess-19-409-2015, 2015.

Page 13, Line 7-9, Supplement Table S3 Please add the values for each of the initial conditions.

Reply: Thank you for your suggestion. We have added the values for the initial conditions into Table S3.

Table S3. Information on model initial conditions

Initial conditions	Description	Unit	Initial value
CWS_{in}	Initial canopy water storage	m	0
SWS_{in}	Initial soil water storage	m	0.5
T_{s0}	Initial surface temperature	℃	T_a
T_{d0}	Initial deep soil temperature	℃	T_a

Results

Page 15, Section 4.1 Not sure whether I overlooked this, but can you please indicate the values of the calibrated parameters? Also: I like Fig 4 showing the objective function. Near the pareto optimum plot a number of potentially very good model runs. Are they all roughly similar parameter values or do they differ substantially? This would give an indication of how well defined this model is in terms of the processes that are represented or/and the sensitivity of some of the parameters. Can you comment on this?

Reply: Thank you for your suggestion. The values of calibrated parameters are shown in L25-26 on P16. But to make it clearer, we also added the calibrated values of parameters directly to the figure caption (L6 on P17).

Regarding whether optimized parameter values are similar or different, we have added the analysis on the optimized parameter values in supplementary Figure S1. C_{veg} and SWS_{max} show low variation of coefficients (CVs), and this indicates the parsimony of the SVEN model. Meanwhile, C_{sat} and b show relatively higher CVs. This may be due to equifinality between C_{sat} and b, which relate to soil thermal properties (Eq. 8) and could compensate each other.

Page 15 Lines 19-20, Page 18, Lines 16-20. I feel the numbers are crowding the text, and are difficult to take in. It is enough to refer to Fig 5, Fig 7 or alternatively collect them in a Table.

Reply: Thank you for your suggestion. We have streamlined these texts. Here we only put the performance regarding RMSDs in the text. Other statistic indices have been moved to Table 3 and Figure 8.

Page 16, Line 5, Line 8 To me Ts does not appear to be underestimated only in high NDVI conditions. Ts is also underestimated in May, when GPP is still very low. I am not convinced of this distinction .. but in order to support your point, you could color the points in the top right panel of Fig 5 with shades indicating NDVI (or GPP).

Reply: Thank you for your suggestion. We have revised Figure 7 to be the boxplot showing the simulation residuals and NDVI. We have also improved the interpretation of results. We agree that the model tends to overestimate Ts for most cases. For details, please refer to L14-16 on P17.

Page 16, Line 24, Fig 5 Would be good to indicate the times of the seven snapshots in Fig 5 by vertical lines (solid for all UAS, dashed for augmented with tower data), so it is easier to see when the data was obtained for calibration.

Reply: Thank you for your suggestion. We have revised Fig 6 (original Fig 5) by adding vertical lines to show the UAS observations. Please see L5 on P18 in the revised version.

Page 16, Line 28 Do you mean "nearby“ instead of "nearly“?

Reply: Thank you for your suggestion. We have revised this sentence. Please see L16 on P19 in the revised version.

Page 18, Line 1 I think "be“ should be erased

Reply: Thank you for your suggestion. We have erased “be” and revised this sentence.

Page 18, Line 4-5, Fig 6 Can you please indicate in Fig 6 what the red lines refer to? I am at a loss, especially in panel (a). Also, I am not sure how the conclusion "GPP was underestimated under diffuse radiation conditions“ is seen from the Figure, I am assuming in panel (j). Does the point cloud show a trend?

Reply: Thank you for your suggestion. The red lines in Fig 6 refers to that the model simulation residuals are equal to 0. To make this clear, we have added detailed explanation to the caption. Please see L4 on P20. In addition, we have revised the original scatter plots to the boxplots, which could be clearer to identify how the model simulation performance changes with NDVI and radiation conditions.

Page 18, Line 6 Add "of‘ after enhancement

Reply: Thank you for your suggestion. We have revised this sentence to make it clear. Please see L7 on P20 in the revised version.

Fig 7 Fonts in the top and bottom panels are not the same. Fig 5 & Fig 7 I was confused at first about the difference of the Fig 7 to the right panels in Fig 5. I concluded they are the same, just showing different time intervals. Can you collect them in one Fig? It would be easier to compare.

Reply: Thank you for your suggestion. To make figures clear, we have revised the figure to make fonts consistent. In addition, we have merged Fig 7 and Fig 5. Please see L1-6 on P21 in the revised version.

Reviewer 3:

Response to the review of Referee 3. We have copied the comments of the referee hereunder with our comments appearing after the referee's comments.

1. General comments

"Temporal interpolation of land surface fluxes derived from remote sensing – results with an Unmanned Aerial System" describes the use of a suite of simple models to interpolate surface fluxes and surface state variables between sporadically available land surface measurements. A model dubbed the SVEN was created by augmenting a Priestly Taylor model with new components to enable its use at timescales as short as 30-min. Instantaneous remotely sensed variables recorded mainly using a UAS were used to calibrate the model, and the model was then used to fill in the extensive gaps between measurements. This work introduces and demonstrates of the technique, which was designed to be used with both satellite and UAS remote sensing measurements. It is a solid manuscript, with room for some improvement.

Because one of the primary stated goals of the paper is the development of an application to satellite remote sensing, the omission of actual satellite measurements is conspicuous. I suggest that more attention be given to the topic of using satellite data. For example, what might be the shortcomings of applying the model to satellite-based measurements? Were UAS measurements relied upon for this paper rather than space-based measurements due to the inadequate spatial resolution of satellite measurements? At this site in-situ and UAS measurements are available (and used), but how well will the model work for the rest of the Earth's surface? Clarify the purpose of the model (including the parameter fitting) in the broadest sense, and develop, test, and describe the results accordingly.

In addition, more care needs to be taken with the way remotely sensed measurements are handled. They are misleadingly referred to as "ground truth" or direct measurements throughout the manuscript, when most of the variables derived from remote sensing data were modeled or inferred, rather than measured directly. Uncertainties due to this also require more attention.

The writing should be reviewed carefully by a native English speaker. Some examples are included in the specific comments below, but the manuscript includes many errors in writing and sentence structure.

Reply: We appreciate the reviewer's insightful comments and suggestions, which were very helpful to improve the manuscript. We totally agree that the great potential of utilizing the simple but effective land surface models to fill gaps between observed surface states and fluxes from remote sensing. We have thoroughly revised the manuscript to improve the presentation of this work. We have also added the discussion on the shortcomings of applying this model to satellite-based measurements and the rest of the Earth's surface. For instance, the SVEN model is a very simple water balance model, which has limited capacity to simulate soil water dynamics particularly in regions with complex landforms. In our study, SVEN also achieved moderate performance to simulate soil water dynamics. In addition, the soil layer depth refers to the maximum root water uptake depth, which may vary with time, but the model simplified this soil depth parameter to keep it consistent. Thus, in our study, SVEN also achieved moderate performance to simulate soil water dynamics. Meanwhile, the PT-JPL model has the limited performance to simulate ET in the dryland regions. There also remain challenges to get the reliability of atmospheric forcing such as radiation, precipitation and wind speed, particularly for data-scarcity regions. Moreover, the remote sensing based estimates of land surface temperature and soil moisture have

uncertainties, which could be propagated to induce significant errors in the simulated continuous land surface variables. In addition, satellite based observations or estimates can have large uncertainties due to the coarse resolution. The integration of land surface model and satellite earth observation might be challenging than the integration with UAS derived variables. Please find the details in the discussion 4.4 (P22-23).

We have also revised the words on "ground truth". We have changed the words to the UAS derived observations or estimates. We have also thoroughly revised the language and improve the manuscript writing.

Here, we have also addressed your comments point-by-point.

2. Specific comments

P 1, ln 7-8. With the exception of Ts, all of these variables are determined using remote sensing products based on a suite of different models and assumptions. For example, different vegetation indices can be measured remotely, but GPP cannot. The same applies to ET, SM, and Rn – none of these variables are measured directly using remote sensing, but the first sentence misleadingly indicates otherwise. Without detracting from main point of this sentence, a word such as "inferred" or "derived" could easily be included for more accuracy.

Reply: Thank you for your suggestion. We have revised the terminology to use "derived" to indicate that variables such as GPP, ET, SM (θ) and Rn were estimated from remote sensing data.

3. P 1, ln 20. Delete the word, "well" from, "…SVEN can well estimate…". Awkward as written.

Reply: Thank you for your suggestion. We have deleted this word. Please see L20 on P1 in the revised clean version.

4. P 2, ln 2-3. "Minimum parameterization" is awkward as written.

Reply: Thank you for your suggestion. We have deleted these words. Please see L1 on P2.

5. P 2, ln 7. "Mostly needed" is awkward as written. Also, replace "high frequency" with "prevalence."

Reply: Thank you. We have deleted "mostly" and have replaced "high frequency" with "prevalence". Please see L6 on P2 in the revised clean version.

6. P 2, ln 11. Replace "flexibly" and "favorable" with more precise descriptors.

Reply: Thank you. We have revised "flexibly" with "favorably". Please see L10 on P2.

7. P 2, ln 14. Replace "still just provide" with "still only provide."

Reply: Thank you. We have revised "still just provide" with "still only provide". Please see L20 on P2.

8. P 2, ln 16. Replace “uncovered” with “unknown.”

Reply: Thank you. We have revised “uncovered” with “unknown”. Please see L22 on P2.

9. P 2, ln 25. “using statistical interpolation could be challenging…” is awkward as written.

Reply: Thank you. We have revised this sentence to be “the statistical method to interpolate for variables that change substantially at sub-daily or daily time scales in response to the surface energy dynamics, e.g. Ts, Rn, SM, ET and GPP, could be challenging”. Please see L30 on P2.

10. P 2, ln 28-29. “can be better” is awkward as written.

Reply: Thank you. We have revised this sentence to be “has great potential”. Please see L1-2 on P3.

11. P 2, ln 30. Delete “a” in, “in a variable climate conditions.”

Reply: Thank you. We have deleted “a”.

12. P 3, ln 6. “as for example the turbulent fluxes are typically…” is awkward as written.

Reply: Thank you. We have deleted the sentence.

13. P 3, ln 7. “simpler but operational models based interpolation” is awkward as written.

Reply: Thank you. We have revised the sentence to be “Simple model based interpolation can be utilized to interpolate snapshot remote sensing estimates of land surface variables.” Please see L12-13 on P3.

14. P 3, ln 11. Delete “the” at the beginning of this line.

Reply: Thank you. We have deleted that. Please see L14 on P3 in the revised version.

15. P 3, ln 15. Rewrite as, “limited meteorological inputs, and parameters that…”.

Reply: Thank you for your suggestion. We have revised this sentence to be “We aimed at using prescribed vegetation dynamics from EO based vegetation indices, limited meteorological inputs, and parameters optimized from remote sensing derived fluxes to estimate temporally continuous land surface variables”. Please see L19-21 on P3.

16. P3, ln 21-22. “now becomes” is awkward as written.

Reply: Thank you. We have revised the words to be “serve as”. Please see L27 on P3 in the revised clean version.

17. P4, ln 4. Add the word, “it” after “forcing”.

Reply: Thank you. We have added “it” after “forcing”. Please see L10 on P4.

18. P4, ln 17. Change, “onboard have been conducted” to, “onboard were conducted.” And “Details refer…” to, “For more details refer...”.

Reply: Thank you. We have changed the sentence to be “were conducted” and “for details, please refer to”. Please see L22-23 on P4.

19. Figure 1. This is exactly the same as Figure 1 from Wang et al. (2018b). I don’t know HESS’s rules regarding this type of thing, so I will refer to the Editor for guidance. I would never reuse a figure like this myself, but if this is actually acceptable, the original usage should certainly be referenced. In addition, a small wind rose would be a nice addition to the figure; at a measurement height of 10 m (Wang et al., 2018b), the flux footprint will extend well beyond the edges of the figure in some conditions. As an aside to be passed onto the site manager, if the eddy covariance instrumentation were closer to the top of the canopy, it would help alleviate this problem.”

Reply: Thank you for the comment. We don’t want to reuse a figure from another paper. There are several differences between this figure and the one in Wang et al. (2018b). For instance, the new figure used the pseudo-color multispectral imagery (Red: 800 nm, Green: 670 nm, Blue: 530 nm) as the base map, while the one in another paper used a normal RGB photo as the base map. The new figure does not have markers to indicate the samples of soil moisture as Wang et al. (2018b). However, we admit that these two figures are similar. We have revised the figure to have more differences with Wang et al. (2018b). For instance, we have added the wind rose to Figure 1.

Regarding the measurement height, Wang et al. (2018b) did not use CO_2 and water vapor eddy covariance data and the measurement height of 10 m refers to the meteorological observations such as wind speed, solar radiation, and longwave radiation. To make this clear, we have added more explanation to the data section. The CO_2 and water vapor eddy covariance system was adjusted to around 2 m above the maximum canopy height. This means that 2 m (before willow growing) to maximum 4 m (maximum canopy height of 6 m) above zero plane displacement. So, in most cases except for few stable conditions in night, the footprints of eddy covariance did extend beyond the edge of willow plantation. For details, please see L10-15 on P5.

20. P5, ln 24. “Data of few UAS flight campaigns” is awkward as written.

Reply: Thank you for the comment. We have revised this sentence to be "UAS data on June 24th were missing as shown in Table 1". Please see L10 on P6.

21. P5, ln 26. Replace the word, "resemble" with more appropriate verbiage.

Reply: Thank you. We have changed the word to be "simulate". Please see L12 on P6.

22. P5, ln 27. Clarify that the "ground truth" SM measurements were not actual SM measurements, and describe the uncertainty and shortcomings of the remotely sensed SM product in detail.

Reply: Thank you for your suggestion. We have revised the "ground truth" words. For model calibration, the instantaneous values of the T_s and θ estimated from the seven UAS flights were used as reference.

23. P5, ln 29. "which corresponded to the willow emerging period with a high growth rate" is awkward as written.

Reply: Thank you for your suggestion. We have revised this sentence. The minimum revisit time was 10 days in the willow emerging period between May 2nd and May 12th. Please see L14-15 on P6.

24. P7, ln3. "and can facilitates to temporally interpolate" is awkward as written.

Reply: Thank you for your suggestion. We have revised the sentence to "can temporally interpolate the instantaneous land surface variables". Please see L11 on P7.

25. P8, ln 24-26. Clarify that this includes the existence of a canopy. As written, it reads like a simple soil diffusion-based approach, that neglects the existence of vegetation. There is a transfer coefficient for the canopy (Cveg) described on P9, along with LE etc., so I assume this all adds up correctly (I am not a modeler), but a more complete initial description is wanted on P8.

Reply: Thank you for the comment. This model is proposed to simulate GPP and components of evapotranspiration (transpiration, evaporation from the intercepted water, and soil evaporation). Therefore, this model has the vegetation module to calculate the heat exchange between vegetation and ground. To make this clear, we have added more explanations at the beginning of the model description. Please see L16-17 on P7 in the revised clean version.

26. P9, ln 24-25. Change to, "k is the von Karman constant."

Reply: Thank you. We have revised this sentence. Please see L13 on P10.

27. P12, ln 20. "The rest of constraints," is awkward as written.

Reply: Thank you. We have revised this sentence. Other constraints such as thermal regulation reflect changes in LUE due to environmental factors. Please see L9-10 on P13.

28. P12, ln 21. “are the same modifying,” is awkward as written.

Reply: Thank you. We have revised this sentence. “are the same for regulating ETc” Please see L10 on P13.

29. P13, ln 6. Change to, “UAS-derived observations,” or otherwise clarify that many of these UAS variables were not measured directly.

Reply: Thank you. We have revised the sentence. The model inputs of this study were obtained from meteorological data, UAS derived observations or estimates.

30. P14, ln 1. Change, “facilitate,” to, “facilitates.”

Reply: Thank you. We have revised the word. Please see L8 on P15.

31. Eq 34 description. Clarify what time period (e.g. 30 min or 24 h) was used for this EC measurement adjustment, and how missing data were handled.

Reply: Thank you. The EC data energy balance closure errors were corrected at 30 mins using the Bowen ratio approach. We have elaborated this in L18-19 on P15. Regarding the missing data, the data gaps were filled with based on the R-package REddyProc (Wutzler et al., 2018) using the meteorological data as inputs. For details, please refer to L13-15 on P5.

32. P14, ln 25. “well represent” is awkward as written.

Reply: Thank you. We have revised the words to be “the indicators of”. Please see L9 on P16.

33. Validation at the daily time scale Section. Augment the discussion of uncertainty in the UAS-derived measurements (as compared to direct measurements).

Reply: Thank you. We have added the discussion on the uncertainties of UAS derived estimates compared to the direct measurements. Please see L9 on P19.

34. P16, ln 24. “that the better UAS based snapshot estimates of SM…” is awkward as written. Perhaps, “that improving the UAS-based estimates of SM…”.

Reply: Thank you for the comment. We have revised this sentence. Please see L13 on P19.

35. P16, ln 34. “has a large coverage” is awkward as written. More accurately, it could be replaced with something like: “extended well-beyond the edges of the Willow forest of interest”.

Reply: Thank you. We have revised this sentence. During the night time, the eddy covariance footprint extended well-beyond the edges of the willow forest of interest, due to the stable atmospheric conditions. Please see L22 on P19.

36. P18, ln 1. “are be good” is awkward as written.

Reply: Thank you. We have revised this sentence to be “To check the model simulation performance under cloudy conditions”. Please see L6 on P20.

37. P18, ln 3. “do not show difference” is awkward as written.

Reply: Thank you. We have revised this sentence. There were no significant differences for the residuals of the simulated T_s, Rn, SM and LE under low and high diffuse radiation fraction conditions. Please see L7-8 on P20.

38. P18, ln 5. “do to that the model” is awkward as written.

Reply: Thank you. We have revised this sentence to make it clearer. Please see L6-10 on P20.

39. P18, ln 6. “enhancement diffuse radiation effects” is awkward as written.

Reply: Thank you. We have revised this sentence. Please see L6-10 on P20.

40. P18, ln 19. Perhaps change, “R2 for Ts…” to, “R2 for monthly Ts…”

Reply: Thank you. We have revised the sentence to be monthly Ts.

41. P20, ln 10. Change, “understanding on the” to, “understand of the”.

Reply: Thank you. We have revised the words. Please see L7 on P24.

42. Conclusions. What would the effects of using space-based remote sensing measurements be, rather that UAS measurements? Also discuss how well this method will work in areas where in-situ measurements are unavailable to better parameterize the UAS and SVEN measurements.

Reply: Thank you for your comments. We think there would be four major effects of using space-borne remote sensing measurements rather than UAS measurements. First of all, the space-borne remote sensing data have much coarser spatial resolution. If we move the simulation to the large scale with satellite data, we need to find accurate gridded meteorological data as forcing. UAS imagery has limited coverage and thus this study only used one meteorological station data as forcing.

As satellite data have coarser pixel sizes, we also need to consider the sub-grid heterogeneity and identify the effective values for model parameters. Note all parameter values of models were obtained from parameter calibration with remote sensing based estimates. For instance, in our study, we used the look-up tables with soil texture information to identify soil parameter values. In the large-scale simulation with satellite data, the plant functional type and soil type parameterization scheme for different ecosystems and environmental conditions would be needed. However, the integration of accurate remote sensing estimates with land surface models would be beneficial to reduce the dependency of plant functional type parameterization scheme and achieve a higher accuracy to predict land surface variables.

In addition, coarse resolution satellite data may have limited accuracy to predict land surface fluxes compared to the detailed UAS data. Applying SVEN with satellite data to large scale, we also need to be careful about the accuracy of remote sensing based estimates and the error propagation from the model inputs to the outputs.

Satellite data in the optical and thermal ranges can only provide observations during the sunny weather conditions. However, the UAS data in this study were collected in both sunny and cloudy conditions. We envision that using satellite based data to calibrate model may lead the model estimates biased towards the sunny conditions.

Regarding the second question on applying this method in areas where in-situ measurements are unavailable to parameterize SVEN, there could be challenges to get reliable estimates of land surface fluxes. As shown in the model implementation of Fig. 4, the major challenges in data-scarcity regions would be lacking meteorological inputs and soil information. Such meteorological variables could be obtained from the online weather forecasting, although these data might not be as good as the standard weather station measurements. Soil parameters (e.g. hydraulic conductance, soil wilting point, and saturated soil moisture) could be obtained from soil texture maps or using model calibration with remote sensing based soil moisture estimates. For example, the soil moisture with high frequency across the entire growing season could be very helpful to identify the soil wilting point and saturated soil moisture, which could be close to the minimum and maximum values of soil moisture time series respectively. We also admit that estimating land surface fluxes in the data-scarcity regions is challenging and our proposed approach could potentially have more uncertainties compared to the performance in the regions with rich in-situ measurements. But we believe using the remote sensing data from satellites or UAS can facilitate the prediction of land surface fluxes in data-scarcity regions.

We want to keep the conclusion streamlined, so we have added the content into the discussion part to address the potential challenges for applying such methodology to satellite data and data-scarcity regions. Please see L8-34 on P23 in the revised version.

43. Equation and variable abbreviations. I cheated and read the other Reviewer Comments. I disagree with Referee #2 regarding their objection to the use of multiple letter abbreviations; I am already familiar with LUE, PAR, GPP, ET, etc., so their usage made it easier for me to follow the manuscript. In addition (this may have more to with my background than what is most suitable for HESS), I am

more accustomed to Θ than SM for soil moisture, and R (surface runoff) could easily be confused for respiration (although honestly I am not sure if there is a more widely used abbreviation for runoff).

Reply: Thank you for your suggestions. We agree that using abbreviations such as LUE, PAR, GPP and ET would be better for the readers. We have revised some variable abbreviations to make them easier for readers. For instance, in the revised version, we have used Q_s to stand for surface runoff. We have used θ to represent soil moisture. Furthermore, we have also summarized all abbreviations in the supplementary material.

Temporal interpolation of land surface fluxes derived from remote sensing - results with an Unmanned Aerial System

Sheng Wang[1], Monica Garcia[1,2], Andreas Ibrom[1], Peter Bauer-Gottwein[1]

[1]Department of Environmental Engineering, Technical University of Denmark, 2800 Kgs. Lyngby, Denmark
[2]International Research Institute for Climate and Society, The Earth Institute, Columbia University, Palisades, NY, USA

Correspondence to: Sheng Wang (shengwang12@gmail.com), Monica Garcia (mgarc@env.dtu.dk)

Abstract. Remote sensing imagery can provide snapshots of rapidly changing land surface variables, e.g. evapotranspiration (ET), land surface temperature (T_s), net radiation (Rn), soil moisture (SMθ) and gross primary productivity (GPP), for the time of sensor overpass. However, discontinuous data acquisitions limit the applicability of remote sensing for water resources and ecosystem management. Methods to interpolate between remote sensing snapshot data and to upscale them from instantaneous to daily time scale are needed. We developed a dynamic Soil Vegetation Atmosphere Transfer model to interpolate land surface state variables that change rapidly between remote sensing observations. The Soil-Vegetation, Energy, water and CO_2 traNsfer model (SVEN), which combines the snapshot version of the remote sensing Priestley Taylor Jet Propulsion Laboratory ET model and light use efficiency GPP models, incorporates now a dynamic component for the ground heat flux based on the 'force-restore' method and a water balance bucket model to estimate SMθ and canopy wetness at a half-hourly time step. A case study was conducted to demonstrate the method using optical and thermal data from an Unmanned Aerial System in a willow plantation flux site (Risoe, Denmark). Based on model parameter calibration with the snapshots of land surface variables at the time of flight, SVEN interpolated the UAS based snapshots T_s, Rn, SM, ET and GPP to continuous records of T_s, Rn, θ, ET and GPP for the growing season of 2016 with forcing from continuous climatic data and NDVI. Validation with eddy covariance and other in-situ observations indicates that SVEN can well estimate daily land surface fluxes between remote sensing acquisitions with root mean square deviationsnormalized root mean square deviations of the simulated daily T_s, Rn, SMθ, LE and GPP equal to 2.35 °C11.77%, 14.49 W·m^{-2},6.65%, 1.98% m^3·m^{-3},19.53%, 16.62 W·m^{-2}-14.77%, and 3.01 g·C·m^{-2}·d^{-1},12.97%, respectively. This study demonstrates that, in this deciduous tree plantation, temporally sparse optical and thermal remote sensing observations can be used as "ground truth" to calibrate soil and vegetation parameters of a simple land surface modelling scheme to estimate "low persistence" or rapidly changing land surface variables with the use of few forcing variables. This approach can also be applied with remotely sensed data from other platforms to fill temporal gaps, e.g. cloud induced data gaps in satellite observation.

1 Introduction

Continuous estimates of the coupled exchanges of energy, water and CO_2 between the land surface and the atmosphere are essential to understand ecohydrological processes (Jung et al., 2011), to improve agricultural water management (Fisher et al., 2017), and to inform policy decisions for societal applications (Denis et al., 2017). Earth observation (EO) data have been increasingly used to estimate the land surface-atmosphere flux exchanges at the time of sensor overpass ~~with minimum parameterization~~, particularly for regions with scarce ground observations. Optical and thermal remote sensing can provide snapshots of these fluxes such as soil moisture (~~SM~~θ) (Carlson et al., 1995; Sandholt et al., 2002), evapotranspiration (ET) (Fisher et al., 2008; Mu et al., 2013) or gross primary productivity (GPP) (Running et al., 2004) using land surface reflectance or temperature. However, both optical and thermal satellite observations present gaps during cloudy periods, and those gaps may coincide with the time when such information is ~~mostly~~ needed (Westermann et al., 2011), for instance, the ~~high frequency~~prevalence of cloudy weather during the crop growing season in monsoonal regimes (García et al., 2013) and high latitude regions (Wang et al., 2018a). Methods are needed to temporally interpolate and upscale the instantaneous records into continuous daily, monthly or annual ~~values~~estimates (Alfieri et al., 2017; Huang et al., 2016).

As one of the most exciting recent advances in near-Earth observation, Unmanned Aerial Systems (UAS) can ~~flexibly~~favourably fly at a low altitude (< 100-200 m) with ~~favourable~~flexible revisit times and low cost (Berni et al., 2009; McCabe et al., 2017). Compared to satellites, UAS provide opportunities to acquire high temporal and spatial resolution data under cloudy weather conditions to monitor and understand the surface-atmosphere energy, water and CO_2 fluxes (Vivoni et al., 2014). For instance, ~~the~~ two-source energy balance models have been extensively applied with UAS thermal imagery for mapping spatial variability of ET (Hoffmann et al., 2015; Kustas et al., 2018; Nieto et al., 2019). Zarco-Tejada et al. (2013, 2016) applied UAS based hyperspectral and solar-induced fluorescence techniques to infer crop physiological and photosynthesis information. Wang et al. ~~. However, UAS observations still just~~(2018b) utilized the vegetation temperature triangle approach with UAS thermal imagery, multispectral imagery and digital elevation model to derive high spatial resolution information of root-zone soil moisture. Wang et al. (2019a) demonstrated the ability of UAS multispectral and thermal imagery for mapping high spatial resolution ecosystem water use efficiency in a willow ~~field~~plantation. However, UAS observations still only provide snapshots of the land surface status at the time of the flight, while conditions such as land surface temperature (T_s), net radiation (Rn), ~~SM~~θ, ET and GPP between image acquisitions remain ~~uncovered~~unknown.

To continuously estimate land surface-atmosphere energy, water and CO_2 fluxes, remote sensing based observations or simulations require either statistical or process-model based approaches to be interpolated into continuous records. The statistical approach is often used to interpolate those land surface variables with ~~low~~high persistence, e.g., which do not change rapidly and can be assumed to be static ~~during~~for several days. For instance, to exclude cloud influence for proxies of vegetation structure e.g. vegetation indices (VI), satellite products use pixel composites to take the maximum value of VI from a given period between 8 and 16 days. To fill the gaps for this period, these 8 or 16 day maximum VI can be statistically interpolated into daily or sub-daily time series data, as the vegetation growth does not change significantly

during such a short period. However, ~~for~~the statistical method to interpolate variables that change substantially at sub-daily or daily time scales in response to ~~changes in~~ the surface energy ~~balance~~dynamics, e.g. T_s, Rn, ~~SM~~θ, ET and GPP, ~~using statistical interpolation~~ could be challenging with low revisit frequency. For instance, Alfieri et al. (2017) found that a return interval of EO observations of no less than 5 days was necessary to statistically interpolate daily ET with relative errors smaller than 20%. To interpolate low persistence variables between remote sensing acquisitions, a dynamic model based interpolation approach considering the dynamics of the land surface energy balance ~~can be better~~has great potential.

Ecosystem and land surface models, which can be used to diagnose and predict ecosystem functioning in ~~a~~ variable climatic conditions, such as BIOME-BGC (Running and Coughlan, 1988) and Simple Interactive Biosphere Model (SiB2, Sellers et al., 1996), can be used to temporally interpolate the land surface fluxes between EO snapshots with available model drivers and parameter values. Djamai et al. (2016) combined Soil Moisture Ocean Salinity (SMOS) Disaggregation, which is based on the Physical and Theoretical Scale Change (DisPATCh) downscaling algorithm, with the Canadian Land Surface Scheme (CLASS) to temporally interpolate ~~SM~~θ at very high spatial and temporal resolutions. Malbéteau et al. (2018) used the ensemble Kalman filter approach to assimilate DisPATCh into a simple dynamic model to temporally interpolate ~~SM~~θ. Jin et al. (2018) temporally interpolated AMSR-E based ~~SM~~θ estimates with the China Soil Moisture Dataset (SCMD) from the Microwave Data Assimilation system. However, temporal interpolation using complex land surface models requires large data inputs and complicated parameterization schemes~~, as for example the turbulent fluxes are typically modelled using mass transfer approaches.~~. In view of these challenges, ~~simpler but operational models~~ simple model-based interpolation can be ~~derived for~~utilized to interpolate snapshot remote sensing ~~models~~estimates of land surface variables. For instance, using a one-dimensional heat transfer equation, Zhang et al. (2015) interpolated ~~the~~ daily T_s on cloudy days. Based on surface energy balance (SEB), Huang et al. (2014) proposed a generic framework with two to twelve parameters to temporally interpolate satellite based instantaneous T_s to diurnal temperatures for ~~the~~ clear sky conditions with mean absolute errors from 1.71 to 0.33 °C, respectively. However, model based approaches to temporally interpolate various land surface fluxes such as ET and GPP are rare.

This study aims at developing a simple but operational land surface modeling scheme, which simulates the land surface energy balance and water and CO_2 fluxes between the land surface and the atmosphere. We aimed at using ~~EO based~~ prescribed vegetation dynamics from EO based vegetation indices, limited meteorological inputs, and parameters ~~which can be~~ optimized from remote sensing derived fluxes~~.~~ to estimate the temporally continuous land surface variables. It can be used for various conditions even in data~~-~~-scarce regions by performing parameter calibration with snapshot remote sensing estimates of T_s, ~~SM~~θ, ET or GPP at the time of overpass. A Soil-Vegetation water and CO_2 flux Exchange, eNergy balance model (SVEN) was developed to continuously estimate T_s, ~~SM~~θ, GPP and ET. The SVEN model is based on a joint ET and GPP model, which combines a light use efficiency GPP model and the Priestley–Taylor Jet Propulsion Laboratory ET model (Wang et al., 2018a). This joint ET and GPP diagnostic model can simulate canopy photosynthesis, evaporation of intercepted water, transpiration and soil evaporation with EO data as inputs. This model ~~now becomes~~serves as a part of the

transient surface energy balance scheme, SVEN, which incorporates additional processes and interactions between soil, vegetation and atmosphere, e.g. surface energy balance, sensible heat flux, and ~~SM~~θ dynamics, to be able to simulate the land surface fluxes when EO data are not available. Compared to most traditional land surface models, which couple processes of transpiration and CO_2 exchange through stomata behaviour and use a 'bottom-up' approach to upscale processes from the leaf scale to the canopy scale (Choudhury and Monteith, 1988; Shuttleworth and Wallace, 1985), SVEN uses a 'top-down' approach to directly simulate water and CO_2 fluxes at the canopy scale. SVEN estimates GPP and ET under potential or optimum conditions and then the potential values are down-regulated by the same biophysical constraints reflecting multiple limitations or stresses. These constraints can be derived from remote sensing and atmospheric data (García et al., 2013; McCallum et al., 2009). In this way, SVEN avoids detailed descriptions and parameterization of complex radiation transfer processes at the leaf level and the scaling process to the canopy level. It maintains a level of complexity comparable to that of operational remote sensing based GPP and ET instantaneous models while being able to predict the fluxes in periods without EO data.

The main objective of this study was to demonstrate a methodology to temporally interpolate sparse snapshot estimates of land surface variables into daily time steps relying on UAS observations. Specific objectives were (1) to develop an operational 'top-down' model to simulate rapidly changed variables e.g. T_s, Rn, ~~SM.~~θ, ET and GPP to interpolate between remote sensing snapshot estimates; (2) to demonstrate the application of this model with UAS observations, calibrating the model with UAS snapshot estimates and forcing it with meteorological data and statistically interpolated VI.

2 Study site and data

2.1 Study site

This study was conducted in an eddy covariance flux site, Risoe (DK-RCW), which is an 11-hectare willow bioenergy plantation adjacent to the DTU Risoe campus, Zealand, Denmark (55.68°N, 12.11°E), as shown in Figure 1. This site has a temperate maritime climate with the mean annual temperature ~~around~~of about 8.5°C and precipitation of around 600 $mm \cdot yr^{-1}$. The soil texture of this site is loam. The stand consists of two clones ('Inger' and 'Tordis') ~~from~~ crossing of *Salix viminalis*, *Salix schwerinii* x *Salix triandra*. In February of 2016, the aboveground parts were harvested following the regular management cycle. Then willow trees grew to a height of approximately 3.5m during the growing season of 2016 (May to October). Rapeseed (*Brassica napus*) was grown in the nearby field. A grass bypass is between the willow plantation and the rapeseed field. An eddy covariance observation system (DK-RCW) has been operated since 2012. Regular UAS flight campaigns with a multispectral camera (MCA, Multispectral Camera Array, Tetracam, Chatsworth, CA, USA) and a thermal infrared camera (FLIR Tau2 324, Wilsonville, OR, USA) onboard ~~have been~~were conducted in this site during the growing seasons of 2016. ~~Details~~For more details, please refer to Wang et al. (2018b).

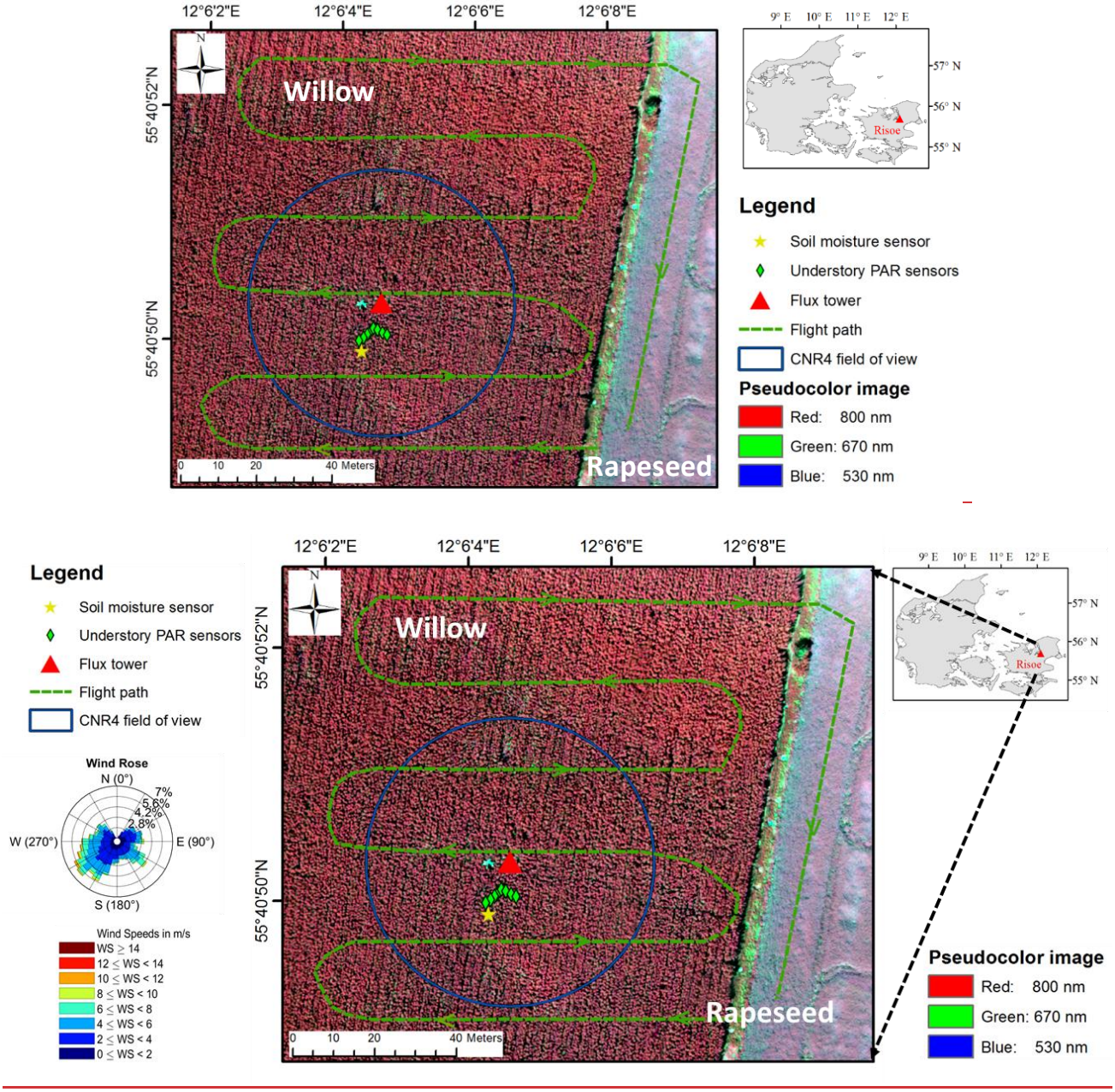

Figure 1. Overview of the Risoe willow plantation eddy covariance flux site. The flux tower is the red triangle in the middle of the willow plantation. The green dashed line shows the typical flying path of UAS. Green diamonds indicate the location of the understory PAR sensors. The yellow star ~~is~~refers to the ~~location of~~ soil moisture sensor. The blue circle indicates the CNR4 field of view. The wind rose refers to the wind conditions in 2016. The base map is a multispectral pseudo-colour image collected on August 1st, 2016 with 800, 670 and 530 nm as red, green and blue channels, respectively.

2.2 Data

In-situ data used in this study include standard eddy covariance and micrometeorological observations, such as GPP, ET, Rn, incoming longwave radiation (LW_{in}), outgoing longwave radiation (LW_{out}) and incoming shortwave radiation (SW_{in}), air temperature (T_a), vapor pressure deficit (VPD) and ~~SM~~θ. These meteorological variables were measured at the height of 10 m above the ground. Meanwhile, the CO_2 and water vapor eddy covariance system was adjusted to around 2 m above the maximum canopy height. The eddy covariance data processing followed the same procedures as in Pilegaard et al. (2011), Ibrom et al. (2007) and Fratini et al. (2012), i.e. the standard ICOS processing method. The raw data were aggregated into half ~~-~~hourly records. The flux partitioning to separate GPP and respiration was done by the look-up table approach (Reichstein et al., 2005) based on the R-package REddyProc (Wutzler et al., 2018) with the half-hourly net ecosystem exchange, T_a and SW_{in} as inputs.

~~An~~A UAS equipped with MCA and FLIR cameras was used to collect the Normalized Difference Vegetation Index (NDVI) and land surface temperature (T_s) (Wang et al., 2019). For each flight campaign, the digital surface model (DSM), multispectral reflectance and thermal infrared orthophotos were generated. For details on the UAS, sensors and image processing, refer to Wang et al. (2018b). To continuously estimate the land surface fluxes from UAS, the collected mean NDVI for the willow patch was temporally statistically interpolated into half-hour continuous records by the Catmull-Rom spline method (Catmull and Rom, 1974). The interpolated NDVI was converted into the fraction of intercepted photosynthetically active radiation (f_{IPAR}), which can also be assumed equal to the fraction of vegetation cover~~,~~ based on Fisher et al. (2008). The canopy height h_c was obtained from the DSM generated from RGB images and then was statistically interpolated into the continuous half-hourly record based on in-situ f_{IPAR}. The collected T_s and NDVI from UAS were used to estimate ~~the volumetric SM~~θ based on the modified temperature-vegetation triangle approach as Wang et al. (2018b). Values of the observed NDVI, T_s and the estimated ~~SM~~θ from each UAS flight campaign are shown in Table 1. The statistically interpolated NDVI and h_c were used as model inputs/forcing.

~~Due to technical issues,~~As technical issues, parts of UAS data ~~of few UAS flight campaigns~~on June 24th and August 1st ~~-~~were missing ~~(as shown in T~~Table 1~~)~~ and~~.~~ ~~The observed data from the~~ in-situ measurements were used to represent these missing values. For instance, ~~T~~to fill a prolonged gap for UAS observations in June of 2016 and ~~resembles~~simulate the growth process of willow trees, ~~a data point based on~~ in-situ observations w~~ere~~as added to June 24th. For model calibration, the instantaneous values of the T_s and ~~SM~~θ estimated from the seven UAS flights were used as ~~"ground truth" or observations~~reference. The seven UAS flights resulted in an average frequency of 25 days for this growing season. The minimum revisit time was 10 days in the willow emerging period between May 2nd and May 12th~~, which corresponded to the willow emerging period with a high growth rate~~. The maximum revisit time was 67 days between August 1st to October 7th when the willow canopy was dense and stable.

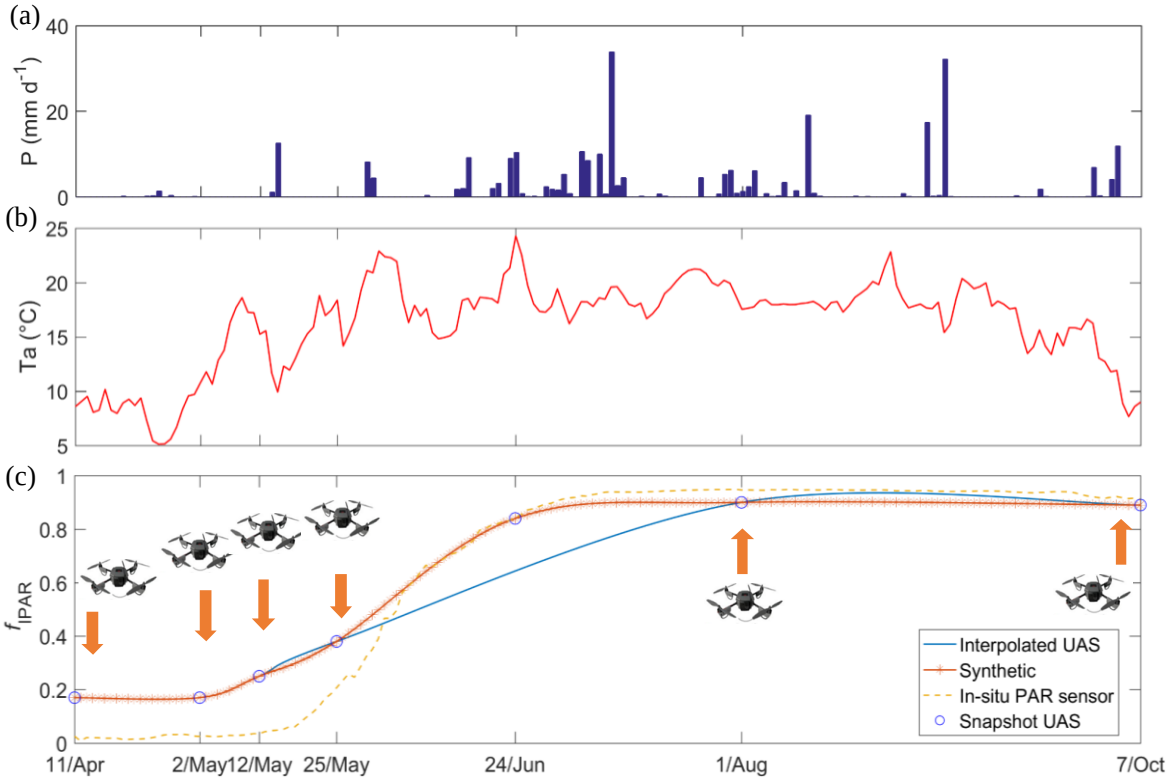

Figure 2. (a) Daily precipitation (P, mm·d^{-1}), (b) Daily air temperature (T_a, °C), and (c) Daily fraction of the intercepted PAR (f_{IPAR}) interpolated from UAS based NDVI during the growing season of 2016.

Table 1. NDVI, ~~LST~~ surface temperature and ~~SM~~soil moisture information from UAS and in-situ data. * indicates that no available data from UAS due to technical issues and ~~the~~ in-situ data were used to represent ~~the~~ UAS snapshots. f_{IPAR} is the fraction of ~~the~~ intercepted PAR. T_s is ~~the~~ land surface temperature (°C). θ is ~~the~~ volumetric ~~SM~~soil moisture ($m^3 \cdot m^{-3}$). For methods ~~on SM~~of θ estimation and detailed weather conditions, please refer to Wang et al. (2019b).

Date	Acquisition time	Weather	f_{IPAR} UAS	f_{IPAR} obs	T_s UAS	T_s obs	θ UAS	θ obs	Growth stage
11-Apr-16	11:13-11:26	Cloudy	0.22	0.03	14.98	15.95	0.27	0.28	Early growth
2-May-16	14:40-14:55	Cloudy	0.22	0.03	18.29	19.13	0.27	0.30	Early growth
12-May-16	10:44-11:55	Sunny	0.3	0.04	24.84	23.57	0.25	0.27	Early growth
25-May-16	10:11-10:23	Sunny	0.43	0.20	28.08	28.31	0.26	0.26	Early growth
24-Jun-16	12:00-12:30	Sunny	0.84*	0.84	26.60*	26.60	0.21*	0.21	Dense vegetation
1-Aug-16	10:06-10:14	Cloudy	0.95	0.95	18.33*	18.33	0.20*	0.20	Dense vegetation
7-Oct-16	11:41-11:55	Sunny	0.94	0.91	11.10	10.41	0.16	0.19	Dense vegetation

3 Method

The SVEN model is an operational and parsimonious remote sensing based land surface modeling scheme expanding the capabilities of the remote sensing GPP and PT JPL-ET model (Wang et al., 2018a) to be dynamic. It runs at half-hourly time steps and can ~~facilitates to~~ temporally interpolate the ~~simulated~~ instantaneous land surface variables, such as T_s, Rn, ~~SM~~θ, ET and GPP, into continuous records.

3.1 Model description

SVEN consists of a surface energy balance module, a water balance module and a CO_2 flux module. In the energy balance module, SVEN estimates the surface temperature and ground heat flux relying on the land surface energy balance equations and the 'force-restore' method (Noilhan and Mahfouf, 1996; Noilhan and Planton, 1989) to consider the energy exchange between ground and soil/vegetation on surface. The water balance module includes the Priestley–Taylor Jet Propulsion Laboratory (PT-JPL) model for ET estimation and a simple 'bucket' model representing the upper soil column to simulate soil water dynamics and runoff generation. The CO_2 flux module uses a light use efficiency (LUE) model for GPP estimation, which is connected to ET via the same canopy biophysical constraints. Figure 3 shows the major processes simulated in SVEN. Detailed information on these three modules is outlined below.

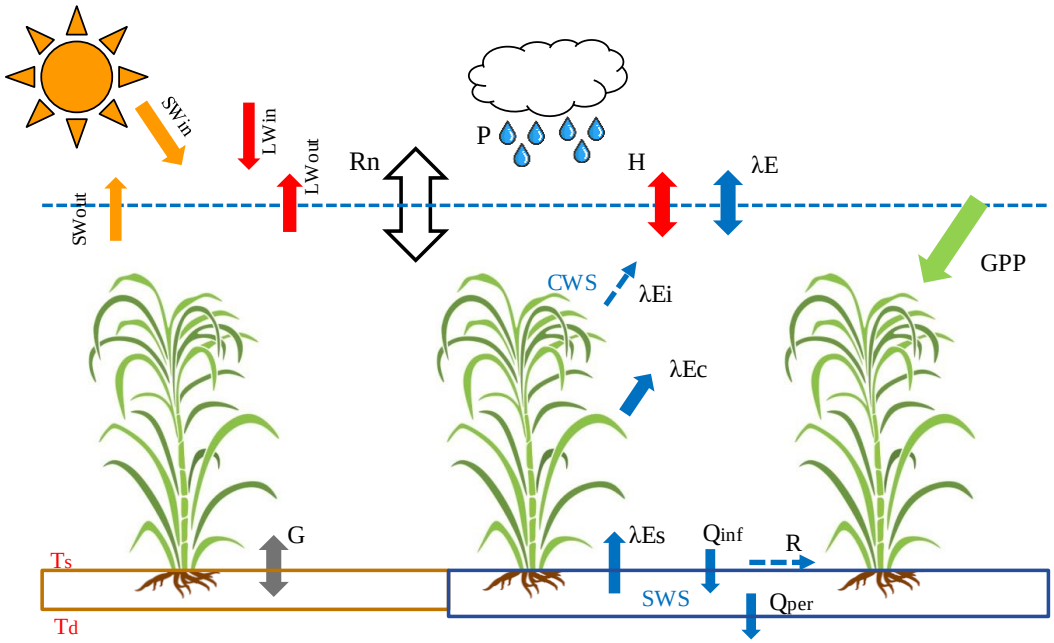

Figure 3. Major land surface processes simulated in SVEN. These processes include land surface energy balance, water fluxes and CO_2 assimilation (SW_{in}: incoming shortwave radiation; SW_{out}: outgoing shortwave radiation; LW_{in}: incoming longwave radiation; LW_{out}: outgoing longwave radiation; Rn: net radiation; G: ground heat flux; T_s: the surface temperature;

T_d: the deep soil temperature; H: sensible heat flux; P: precipitation; λE: latent heat flux; λEi: latent heat flux of the intercepted water; λEc: latent heat flux of transpiration; λEs: latent heat flux of soil evaporation; CWS: canopy water storage; SWS: soil water storage; Q_{inf}: infiltration; Q_{per}: percolation; R: surface runoff; GPP: gross primary productivity.

3.1.1 Surface Energy Balance Module

The instantaneous net radiation is estimated based on the surface energy balance, as shown in Eq. (1). The surface emissivity is approximated according to an empirical relation with NDVI as Eq. (2) (Van de Griend and M.Owe., 1993). The surface albedo (~~ALB~~A) is estimated from the simple ratio vegetation index (SR) and it shows that albedo generally decreases as vegetation greenness increases as Eq. (3 and 4) (Gao, 1995).

$$Rn = \text{~~(1 − ALB)~~}(1 - A)SW_{in} + (1 - \varepsilon)LW_{in} - \varepsilon\sigma T_s^4 \quad (1)$$

$$\varepsilon = \begin{cases} 0.986 & (NDVI > 0.608) \\ 1.0094 + 0.047 \cdot \ln(NDVI) & (0.131 < NDVI < 0.608) \\ 0.914 & (NDVI < 0.131) \end{cases} \quad (2)$$

$$\text{~~ALB~~}A = 0.28 - 0.14e^{(-6.08/SR^2)} \quad (3)$$

$$SR = (1 + NDVI)/(1 - NDVI) \quad (4)$$

Where Rn is the instantaneous net radiation ($W \cdot m^{-2}$). SW_{in} is the instantaneous incoming shortwave radiation ($W \cdot m^{-2}$). LW_{in} is the instantaneous incoming longwave radiation ($W \cdot m^{-2}$). σ is the Stefan-Boltzmann constant (5.670367×10^{-8} $W \cdot m^{-2} \cdot K^{-4}$).

At the surface, Rn is dissipated as latent, sensible and ground heat fluxes, as Eq. (5). The latent heat flux is estimated from the PT-JPL ET model and the sensible heat flux, H, is calculated based on the temperature gradient between the surface and air and a bulk aerodynamic resistance. The instantaneous ground heat flux G is estimated from the ´force-restore´ method (Noilhan and Planton, 1989).

$$\frac{dS}{dt} = SW_{in} - SW_{out} + LW_{in} - LW_{out} - H - \lambda E - G \quad (5)$$

Where $\frac{dS}{dt}$ is the heat storage change over time ($W \cdot m^{-2}$). SW is shortwave radiation ($W \cdot m^{-2}$) and LW is longwave radiation ($W \cdot m^{-2}$). The subscripts $_{in}$ and $_{out}$ refer to incoming and outgoing, respectively. λE represents the latent heat flux ($W \cdot m^{-2}$). H refers to the sensible heat flux ($W \cdot m^{-2}$). G is the ground heat flux ($W \cdot m^{-2}$).

The surface temperature was estimated by the 'force-restore' method, which considers two opposite effects on surface temperature variabilities, as shown in Eq. (6). The first term ($R_n - \lambda E - H$) represents the forcing from the surface-atmosphere interface. The second term ($T_s - T_d$) is the gradient between the surface temperature and deep soil temperature. It indicates the tendency from the deep soil to restore T_s (responding to surface energy forcing) to the T_d value, which is more stable over time.

$$\frac{dT_s}{dt} = C_T(R_n - \lambda E - H) - C_d(T_s - T_d) \quad (6)$$

$$\frac{dT_d}{dt} = \omega(T_s - T_d) \quad (7)$$

$$\frac{1}{C_T} = \frac{1-f_c}{C_{sat}(\frac{SWS_{max}}{SWS})^{\frac{b}{2\ln(10)}}} + \frac{f_c}{C_{veg}} \quad (8)$$

$$C_d = 2\pi\omega \quad (9)$$

Where T_s is the land surface temperature (°C). T_d ~~is~~refers to the deep soil temperature (°C) calculated by applying a low-pass filter to T_s~~.~~ with the cut-off frequency of 24 hours. ω is the frequency of oscillation 1/24 (h^{-1}). C_T is a force-restore thermal coefficient for the surface heat transfer ($K \cdot m^2 \cdot J^{-1}$) and is influenced by the effective relative ~~SM~~θ. C_{sat} is the force-restore thermal coefficient for saturated soil ($K \cdot m^2 \cdot J^{-1}$). The parameter b is the slope of the retention curve for the force-restore thermal coefficient. C_{veg} is the force-restore thermal coefficient for vegetation ($K \cdot m^2 \cdot J^{-1}$). f_c is the fractional cover of vegetation and is assumed equal to f_{IPAR} as the supplemental Table S1 (Fisher et al., 2008). SWS_{max} is the maximum soil water storage (~~m^3~~m) and SWS is the actual one (~~m^3~~m). C_d is diurnal periodicity based on ω (h^{-1}).

The sensible heat flux, H, is estimated based on the temperature gradient between the surface and air, as shown in Eq. (10).

$$H = \rho c_p(T_s - T_a)/r_a \quad (10)$$

Where ρ is the air density ($kg \cdot m^{-3}$). c_p is the specific heat capacity of air ($J \cdot kg^{-1} \cdot K^{-1}$). T_s is the land surface temperature (°C). T_a is the air temperature (°C). r_a is the aerodynamic resistance for heat transfer ($s \cdot m^{-1}$).

Aerodynamic resistance to turbulent transport under neutral conditions (r_{aN}) can be expressed as Eq. (11) (Brutsaert, 1982).

$$r_{aN} = \frac{\ln(\frac{z-d}{z_{0m}})\ln(\frac{z-d}{z_{0h}})}{k^2 u} \quad (11)$$

$$d = 0.67h_c \quad (12)$$

$$z_{om} = 0.1h_c \quad (13)$$

$$z_{oh} = \frac{z_{0m}}{e^{kB^{-1}}} \quad (14)$$

Where h_c is the canopy height (m). The parameter d is the zero displacement height (m) and z is the velocity reference height (m). z_{om} is the aerodynamic roughness length for momentum (m). z_{oh} is the aerodynamic roughness length for the heat transfer (m). u is the horizontal wind velocity at reference height ($m \cdot s^{-1}$). kB^{-1} is a parameter to account for the difference between the aerodynamic and radiometric temperatures and a constant value of 2.3 is adopted in this study (Garratt and Hicks, 1973). k is the von Karman constant (0.4).

The aerodynamic resistance is corrected for the atmospheric stability as shown in Eq. (15) (Huning and Margulis, 2015). Ψ_m is the stability correction factor for momentum. Ψ_h is the stability correction factor for sensible heat flux. For unstable conditions (negative temperature gradient), the stability correction factors are less than 1.0 and the correction reduces the resistance and enhances turbulence, while for stable conditions they are greater than 1.0 and the correction increases the resistance and suppresses turbulence.

$$r_a = r_{aN}\Psi_m\Psi_h \quad (15)$$

When the atmospheric condition is unstable ($R_{iB} \leq 0$), Ψ_m and Ψ_h are estimated from Eq. (16).

$$\Psi_h = {\Psi_m}^2 = (1 - 15R_{iB})^{-1/2} \quad (16)$$

When atmospheric condition is stable ($0 \leq R_{iB} < 0.2$), Ψ_m and Ψ_h are estimated from Eq. (17).

$$\Psi_h = \Psi_m = (1 - 5R_{iB})^{-1} \quad (17)$$

$$R_{iB} = \frac{\left(\frac{g}{Ts}\right)\partial Ts/\partial z}{(\frac{\partial u}{\partial z})^2} \quad (18)$$

Where R_{iB} is the bulk Richardson number, g is the gravitational acceleration.

3.1.2 Water balance module

The water balance module simulates evaporation of intercepted water, plant transpiration, soil evaporation, soil infiltration and percolation. The evapotranspiration is estimated based on a modified PT-JPL ET model (Wang et al., 2018a). The PT-JPL ET model has been demonstrated as one of best-performing global remote sensing ET algorithms (Chen et al., 2014; Ershadi et al., 2014; Miralles et al., 2016; Vinukollu et al., 2011). Thus, it was selected for ET estimation. The PT-JPL model (Fisher et al., 2008) uses the Priestley-Taylor (1972) equation to calculate the potential evapotranspiration, and then incorporates eco-physiological variables to down-regulate potential evapotranspiration to actual evapotranspiration. PT-JPL is a three-source evapotranspiration model to simulate evaporation of intercepted water (Ei), transpiration (Ec) and soil evaporation (Es) as following equations.

$$\lambda ET = \lambda Ei + \lambda Ec + \lambda Es \quad (19)$$

$$\lambda Ei = f_{wet} \cdot \alpha\Delta/(\Delta + \gamma) \cdot Rnc \quad (20)$$

$$\lambda Ec = (1 - f_{wet}) \cdot f_g \cdot f_M \cdot f_{Ta} \cdot \alpha_c\Delta/(\Delta + \gamma) \cdot Rnc \quad (21)$$

$$\lambda Es = \sout{f_{SM}} f_\theta \cdot \alpha\Delta/(\Delta + \gamma) \cdot (Rns - G) \quad (22)$$

Where λET is the latent heat flux for total evapotranspiration ($W \cdot m^{-2}$), λEi is the latent heat flux due to evaporation of intercepted water ($W \cdot m^{-2}$), λEc is the latent heat flux due to transpiration ($W \cdot m^{-2}$), and λEs is the latent heat flux due to

evaporation of soil water ($W \cdot m^{-2}$). The quantity f_{wet} is the relative surface wetness to partition the evapotranspiration from the intercepted water and canopy transpiration. f_g is the green canopy fraction indicating the proportion of active canopy. f_M is the plant moisture constraint. f_{Ta} is the plant temperature constraint reflecting the temperature limitation of photosynthesis. ~~f_{SM}~~f_θ is the ~~SM~~θ constraint. These constraints vary from 0 to 1 to account for the relative reduction of potential λET under limiting environmental conditions. Rnc and Rns are the net radiation for canopy and soil, respectively. The partitioning of PAR and net radiation between canopy and soil is calculated following the Beer-Lambert law (Supplemental Table S1). G is the ground heat flux. Δ is the slope of saturation vapor pressure versus temperature curve. γ is the psychrometric constant. α is an empirical ratio of potential evapotranspiration to equilibrium potential evapotranspiration (~~PT~~Priestley-Taylor coefficient). The suggested value for α is 1.26 in the PT-JPL model (Fisher et al., 2008).

In the original model, f_{wet} was estimated from air relative humidity (Fisher et al., 2008). In this study, f_{wet} is modified to be defined as a ratio between the actual canopy water storage (CWS) and the maximum canopy water storage (CWS_{max}) as Eq. (23) (Noilhan and Planton, 1989). CWS is the amount of intercepted water and CWS_{max} is the maximum possible amount of intercepted water (mm), taken as 0.2LAI $kg \cdot m^{-2}$ (Dickinson, 1984). f_{wet} depends on both the precipitation rate and LAI, which is more reasonable than only depending on air relative humidity in the original model.

$$f_{wet} = \frac{CWS}{CWS_{max}} \tag{23}$$

In this study, we determined CWS with a prognostic equation (24) with the constraint that CWS is smaller than CWS_{max}.

$$\frac{dCWS}{dt} = f_c \cdot P - Ei \tag{24}$$

Where f_c is the fraction of vegetation cover and here it is assumed to be equal to f_{IPAR} (Fisher et al., 2008). P and Ei are the rainfall rates and evaporation from the intercepted water, respectively ($m \cdot s^{-1}$).

The effective precipitation rate is estimated as the residual of the rainfall rate and change of CWS as Eq. (25).

$$P_e = P - dCWS \tag{25}$$

To simulate the dynamics of water storage in the soil, SVEN uses a simple 'bucket' model. Here the infiltration rate (Q_{inf}) is equal to the effective rainfall rate (P_e), when the soil water is not saturated. Thus, SWS is calculated based on a prognostic equation with a constraint that SWS is smaller than SWS_{max}.

$$Q_{inf} = P_e \tag{26}$$

$$\frac{dSWS}{dt} = Q_{inf} - Ec - Es - Q_{per} \tag{27}$$

When soil water is saturated, SWS is equal to SWS_{max} and surface runoff (~~R~~Q_s) occurs as Eq. ~~28~~29.

$$Q_{inf} = Ec + Es + Q_{per} \tag{28}$$

$$R = P_e Q_s = P_e - Q_{inf} \quad (29)$$

Where SWS is soil water storage (m). P_e, Ec, Es, Q_{per} and $R Q_s$ are the effective rainfall rates, transpiration rates, evapotranspiration rates from soil, percolation rates and surface runoff ($m \cdot s^{-1}$), respectively.

Percolation is estimated by assuming uniform vertical hydraulic gradient and using the Mualem model for hydraulic conductivity of unsaturated soils (Mualem, 1976) as Eq. (30):

$$Q_{per} = K_s \sqrt{\theta_e}(1 - (1 - \theta_e{}^{1/(1-1/n)})^{1-1/n})^2 \quad (30)$$

$$\theta_e = \frac{\theta - \theta_r}{\theta_s - \theta_r} \quad (31)$$

$$\theta = \frac{SWS}{SWS_{max}} \theta_s \quad (32)$$

Where K_s is the saturated hydraulic conductivity ($m \cdot s^{-1}$). n is a fitting parameter depending on the pore size. θ is the volumetric soil moisture ($m^3 \cdot m^{-3}$). θ_e is the effective soil moisture ($m^3 \cdot m^{-3}$). θ_s is the saturated soil moisture ($m^3 \cdot m^{-3}$). θ_r is the residual soil moisture ($m^3 \cdot m^{-3}$).

3.1.3 CO_2 flux module

The photosynthesis in the CO_2 flux module is calculated from a modified light use efficiency (LUE) model (Wang et al., 2018a) linked to the biophysical constraints for canopy transpiration of the PT-JPL model. The LUE GPP model is a robust and widely used method to estimate GPP across various ecosystems and climate regimes (McCallum et al., 2009). The LUE models, e.g. CASA (Potter et al., 1993) or the MODIS algorithm (Running et al., 2004), are based on the assumption that plants optimize canopy LUE or whole canopy carbon gain per total PAR absorbed as originally suggested by (Monteith, 1972) for net primary productivity. The formula of the LUE GPP model used in this study is shown in Eq. (33) and it is partly based on the Carnegie-Ames-Stanford-Approach model (Potter et al., 1993) with modification to include an additional constraint accounting for the fraction of the canopy that is photosynthetically active (Fisher et al., 2008). The rest ofOther constraints reflects changes in LUE due to environmental factors such as thermal regulation (Wang et al., 2018a) reflect changes in LUE due to environmental factors and are the same modifying thefor regulating ETc (Eq. 21).

$$GPP = LUE_{max} \cdot PARc \cdot f_g \cdot f_M \cdot f_{Ta} \cdot f_{VPD} \quad (33)$$

Where LUE_{max} is the maximum LUE ($g \cdot C \cdot MJ^{-1}$). PARc is the daily photosynthetically active radiation (PAR) ($MJ \cdot m^{-2} \cdot d^{-1}$) intercepted by the canopy and it is calculated based on the extinction of PAR within the canopy using the Beer–Lambert law (Supplemental Table S1). f_g is the green canopy fraction indicating the proportion of active canopy. f_M is the plant moisture constraint. f_{Ta} is the air temperature constraint reflecting the temperature limitation of photosynthesis. f_{VPD} is the VPD constraint reflecting the stomatal response to the atmospheric water saturation deficit. All these constraints range from 0 and

1 and represent the reduction of maximum GPP under limiting environmental conditions. For more details, please refer to the supplemental Table S1.

3.2 Model ~~parameter estimation~~implementation

The SVEN model requires shortwave incoming (SW_{in}), longwave incoming (LW_{in}), air temperature (T_a), air pressure (Ps), relative humidity (RH), wind speed (~~WS~~u), precipitation (P), canopy height (z), and vegetation information (NDVI) as inputs (Supplemental Table S2). The model inputs of this study were obtained from meteorological data ~~and~~, UAS derived observations or estimates. The simulation outputs of this model are shown in Supplemental Table S4. The initial conditions for the model include an initial canopy water storage (CWS_{in}), an initial soil water storage (SWS_{in}), initial surface temperature (T_{s0}) and initial deep soil temperature (T_{d0}) as shown in Supplemental Table S3. The initial conditions to run the model (11-April-2016 to 7-October-2016) were obtained by performing spin-up simulations from 11-March-2016 to 11-April-2016. The details of model implementation are shown in Figure 4.

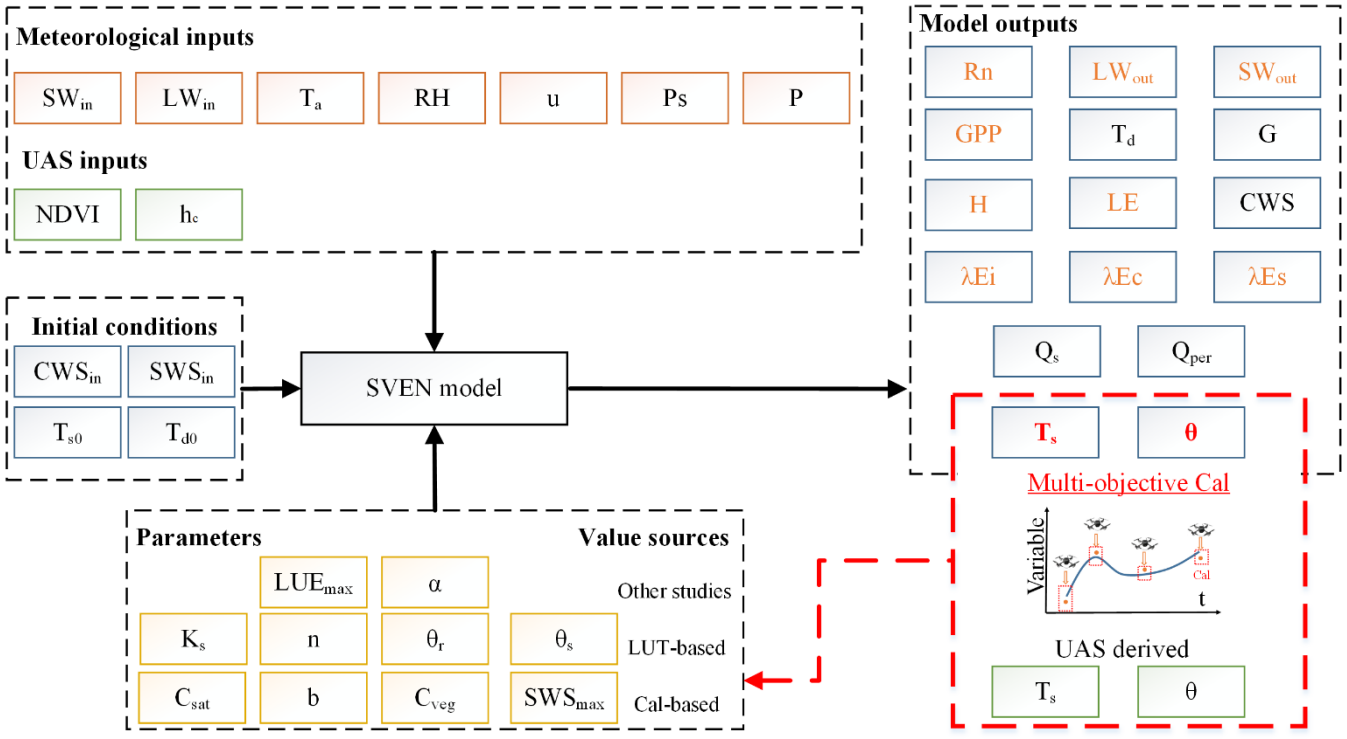

Figure 4. Model implementation of this study. UAS and meteorological data were used as inputs of the SVEN model. Values of the SVEN parameters were obtained from the look-up table, other studies, or model calibration with UAS derived variables. In the model outputs, variables with the highlighted red colour (T_s and θ) refers to the variables calibrated with UAS derived observations or estimates. The variables with orange colours are retrievable from remote sensing techniques.

The SVEN model has six parameters, which are mostly related to physical soil properties for heat transfer and infiltration (Table 2). The parameter values can be obtained from several approaches including look-up tables based on soil texture, parameter values of the similar biome or soil types in other studies, field measurements, or model parameter optimization with in-situ measurements or with remote sensing data. The parameters, for instance maximum light use efficiency (LUE_{max}), to run the snapshot version of SVEN are described in Wang et al., (2018a). As this willow plantation is a deciduous temperate forest, the parameter values obtained from the nearby similar ecosystem (Wang et al., 2018a) were used for this study.

Table 2. Information on the model parameters of SVEN and their ranges for all soil or biome types

Parameters	Description	Unit	Range	Reference	Source for this study
LUE_{max}	Maximum light use efficiency	$g \cdot C \cdot m^{-2} \cdot MJ^{-1}$	0-5	Wang et al. (2018a)	Other studies
α	Priestley-Taylor coefficient	[-]	1-3	Fisher et al. (2018)	Other studies
C_{sat}	The force-restore thermal coefficient for saturated soil	10^{-6} $K \cdot m^2 \cdot J^{-1}$	[3, 15]	Noilhan and Planton (1989)	Model calibration
b	The slope of the retention curve for the force-restore thermal coefficient	[-]	[4.05, 11.4]	Noilhan and Planton (1989)	Model calibration
C_{veg}	The force-restore thermal coefficient for vegetated surface	10^{-6} $K \cdot m^2 \cdot J^{-1}$	[1, 10]	Calvet et al. (1998)	Model calibration
SWS_{max}	Maximum soil water storage	m	[0, 1]	Boegh et al. (2009)	Model calibration
K_s	The infiltration rate for the saturated soil	$mm \cdot h^{-1}$	[0.01, 25]	Dettmann et al. (2014)	Look-up table
n	Fitting parameter of the Mualem model	\	[1, 3]	Dettmann et al. (2014)	Look-up table
θ_s	Soil wilting point	$m^3 \cdot m^{-3}$	[0.38, 0.43]	(Carsel and Parrish, 1988)	Look-up table
θ_s	Saturated soil moisture	$m^3 \cdot m^{-3}$	[0.045, 0.068]	(Carsel and Parrish, 1988)	Look-up table

In this study, we used a combination of these approaches to obtain model parameter values. The fitting parameter of the Mualem model (n) and the infiltration rate for the saturated soil (K_s) were obtained from a look-up table (Carsel and Parrish, 1988). The values for loamy soil as shown in the supplemental Table S5 were used, according to the soil texture of this site. The rest of parameters related with soil and vegetation physical properties, C_{sat}, b, C_{veg} and SWS_{max}, were obtained by calibrating models with instantaneous T_s and ~~SM~~θ from seven UAS flight campaigns (Table 1) rather than calibration with in-situ measurements of ET or GPP (e.g. eddy covariance data) as in other studies. Calibrating the model with the remotely sensed instantaneous estimates instead of ground measurements ~~facilitate~~facilitates the application of this approach to data~~-~~scarce regions. The calibration of C_{sat}, b, C_{veg} and SWS_{max} was conducted using the Monte Carlo optimization. The parameter values were sampled 20,000 times with a uniform distribution and the corresponding parameter ranges as shown in Table 2. The objective function for optimization is the root mean square deviation (RMSD) between the observed and

simulated values. With two objective functions for T_s and ~~SM~~θ respectively, ~~a~~ the multiple objective optimization method (Pareto front) as Yapo et al. (1998) was used to identify the optimized parameter values.

3.3 Model assessment

We used independent eddy covariance data to validate model outputs. However, due to the energy balance closure issue (Wilson et al., 2002), the sum of sensible heat (H) and latent heat (LE) as measured by the eddy covariance method is generally not equal to the available energy (net radiation minus ground heat flux, $R_n - G$). This study used the Bowen ratio approach to correct energy balance closure errors of eddy covariance data. Using~~Assuming~~ ~~that~~ the ratio of 30 min sensible heat to ET (Bowen ratio) ~~is correct~~, LE measurements can be corrected as follows (Twine et al., 2000). The LE data with the 30 min energy balance closure error larger than 20% were excluded in the validation.

$$LE = \frac{R_n - G}{H\_EC\_raw + LE\_EC\_raw} LE\_EC\_raw \quad (34)$$

Where LE is the corrected latent heat by assuming that the Bowen ratio is constant ($W \cdot m^{-2}$). R_n is the net radiation ($W \cdot m^{-2}$). G is the ground heat flux ($W \cdot m^{-2}$). H_EC_raw is the uncorrected sensible heat ($W \cdot m^{-2}$) and LE_EC_raw is the uncorrected latent heat ($W \cdot m^{-2}$).

The SVEN model was developed to interpolate between remote sensing data acquisitions and to produce continuous daily records. Thus, the observed T_s, Rn, LE and GPP are from the eddy covariance system and the in-situ ~~SM~~θ measurements at the depth of 15 cm (the sensor ~~locations shown~~location in Figure 1) were used to validate the simulated variables at the daily time scale. Statistics including RMSD, ~~correlation coefficient~~the coefficient of determination (R^2), ~~and~~ relative errors (RE) and normalized RMSD (NRMSD, the ratio between RMSD and the range of observations) were used in validation.

We also analyzed how the model skill changes depending on vegetation cover and overcast (diffuse radiation) conditions by looking at model residuals as typically remote sensing models may be biased to sunny conditions. Scatterplots between model residuals and NDVI and the diffuse radiation fraction were examined. As the ratio between the actual (SW_{in}) and potential (SW_{in}pot) can ~~well represent~~be the indicator of the diffuse radiation fraction (Wang et al., 2018a), we used this ratio to indicate the diffuse radiation fraction. This analysis can help to understand possible methods to improve the SVEN model. To check the capability of the SVEN model to interpolate half-hourly and monthly time series fluxes, the simulated land surface variables were also validated at half-hourly and monthly time scales, in addition to the daily time scale.

4 Results and discussion

4.1 Model parameter estimation

Figure ~~4~~ 5 illustrates the results of model parameter calibration with UAS ~~based~~derived snapshot ~~SM~~θ and T_s (Table 1). With ~~two~~RMSDs of θ and T_s as objective functions, ~~RMSDs of SM and T_s,~~ a significant trade-off between the performance of ~~the~~

~~SM~~θ and T_s simulations is observed as a Pareto front (the red curve) in Figure 4. The x-axis shows the performance of simulating ~~SM~~θ. The smaller the RMSD values are, the better the model performance with respect to this variable. The minimum, however, lies in a range, where the model performance of the other variable, T_s, is highest (y-axis). From the viewpoint of multi-objective optimization, the solutions at the Pareto front are equally good. By considering RMSDs of T_s less than 2 °C and RMSDs of ~~SM estimates~~θ as small as possible, we selected the point close to the red arrow of Figure 4, which corresponds to the RMSDs of ~~SM~~θ and T_s equal to 2.99% $m^3 \cdot m^{-3}$ and 1.92 °C, respectively. The values of C_{sat}, b, C_{veg} and SWS_{max} at this Pareto front point are equal to 6.94×10^{-6} $K \cdot m^2 \cdot J^{-1}$, 5.20, 2.18×10^{-6} $K \cdot m^2 \cdot J^{-1}$ and 554.52 mm, respectively. Furthermore, we also analysed the variability of optimized parameter values as shown in supplementary Figure S1. C_{veg} and SWS_{max} show low variation of coefficients (CVs), and this indicates the parsimony of the SVEN model. Meanwhile, C_{sat} and b show relatively higher CVs. This may be due to equifinality between C_{sat} and b, which relate to soil thermal properties (Eq. 8) and could compensate each other.

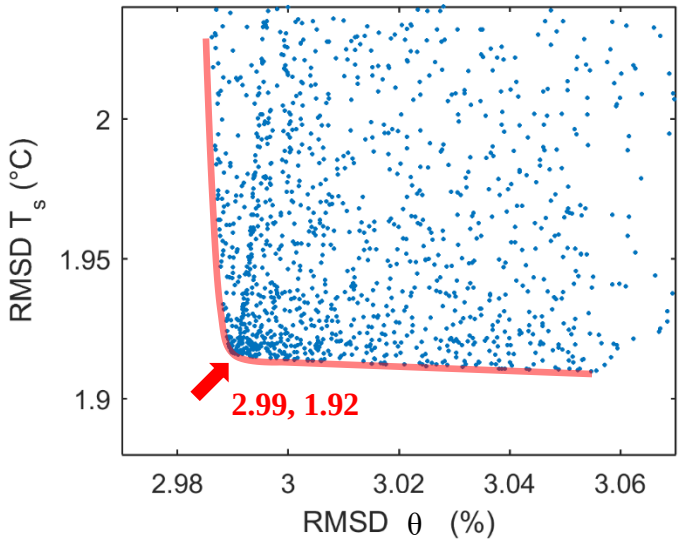

Figure 45. Objective function values of evaluated parameter sets and corresponding Pareto front. The x-axis is the objective function for simulating ~~SM~~θ. The y-axis is the objective function for simulating T_s. Each dot corresponds to one simulation performance. Each of the simulations represents a different combination of candidate parameter sets. The dot closest to the red arrow is chosen to be the optimal parameter set for SVEN continuous simulation. C_{sat}, b, C_{veg} and SWS_{max} at the Pareto front point are 6.94×10^{-6} $K \cdot m^2 \cdot J^{-1}$, 5.20, 2.18×10^{-6} $K \cdot m^2 \cdot J^{-1}$ and 554.52 mm, respectively.

4.2 Validation at the daily time scale

Figure ~~5~~ 6 shows the time-~~-~~series data of the interpolated daily T_s, Rn, ~~SM~~θ, LE and GPP and their validation. ~~It can be seen that the~~ The simulated daily T_s, Rn, ~~SM~~θ, LE and GPP ~~fits~~capture well with ~~observations~~the observed temporal dynamics of

land surface variables at this site. R^2 for daily T_s, Rn, θ, LE and GPP are 0.90, 0.92, 0.50, 0.70 and 0.79, respectively. RMSDs for the simulated daily T_s, Rn, ~~SM~~θ, LE and GPP are 2.35 °C, 14.49 $W \cdot m^{-2}$, 1.98% $m^3 \cdot m^{-3}$, 16.62 $W \cdot m^{-2}$ and 3.01 $g \cdot C \cdot m^{-2} \cdot d^{-1}$, respectively. ~~$R^2$ for T_s, Rn, SM, LE and GPP are 0.90, 0.92, 0.50, 0.70 and 0.79, respectively. RE for T_s, Rn, SM, LE and GPP are 10.47%, -2.96%, -1.05%, 9.23% and -14.53%, respectively. This~~Such simulation accuracy demonstrates that SVEN is capable ~~to temporally interpolate between the remote sensing data acquisitions and interpolate~~of temporal interpolating the snapshot estimates or observations between remote sensing acquisitions to form continuous daily records.

For the simulated T_s, ~~it can be seen that~~ during the early growth stage (before June), the SVEN model simulated quite accurately the temporal dynamics. However, during the dense vegetation stage (high NDVI), the model generally tends to overestimate T_s. Similarly, ~~for~~SVEN underestimated Rn~~,~~ during the early growth stage, ~~the model underestimated Rn, while it~~but overestimated Rn for the dense vegetation stage. These biases can also be identified from the ~~scatterplots between~~boxplots of model residuals and NDVI~~. As shown in Figure 6 (a-b), with low NDVI,~~ (Fig. 7b), which shows that the model underestimates Rn in low NDVI and vice-versa. ~~With high NDVI the simulated T_s shows overestimation.~~ One of the reasons for this error could be the uncertainty in the estimated surface albedo. The albedo in the SVEN model was determined by the simple empirical formula as Eq. (3) with a high value in the early growth stage and a low value for dense vegetation. Another possible source for errors is from uncertainties in C_{veg}, which reflects the thermal storage property of vegetated surface in the force-restore method. C_{veg} was obtained ~~from~~through model calibration with UAS observed T_s. As shown in Figure ~~1~~2, only three UAS data sets were available in the vegetated period. The insufficient model calibration may lead to ~~the~~ uncertainties in C_{veg}.

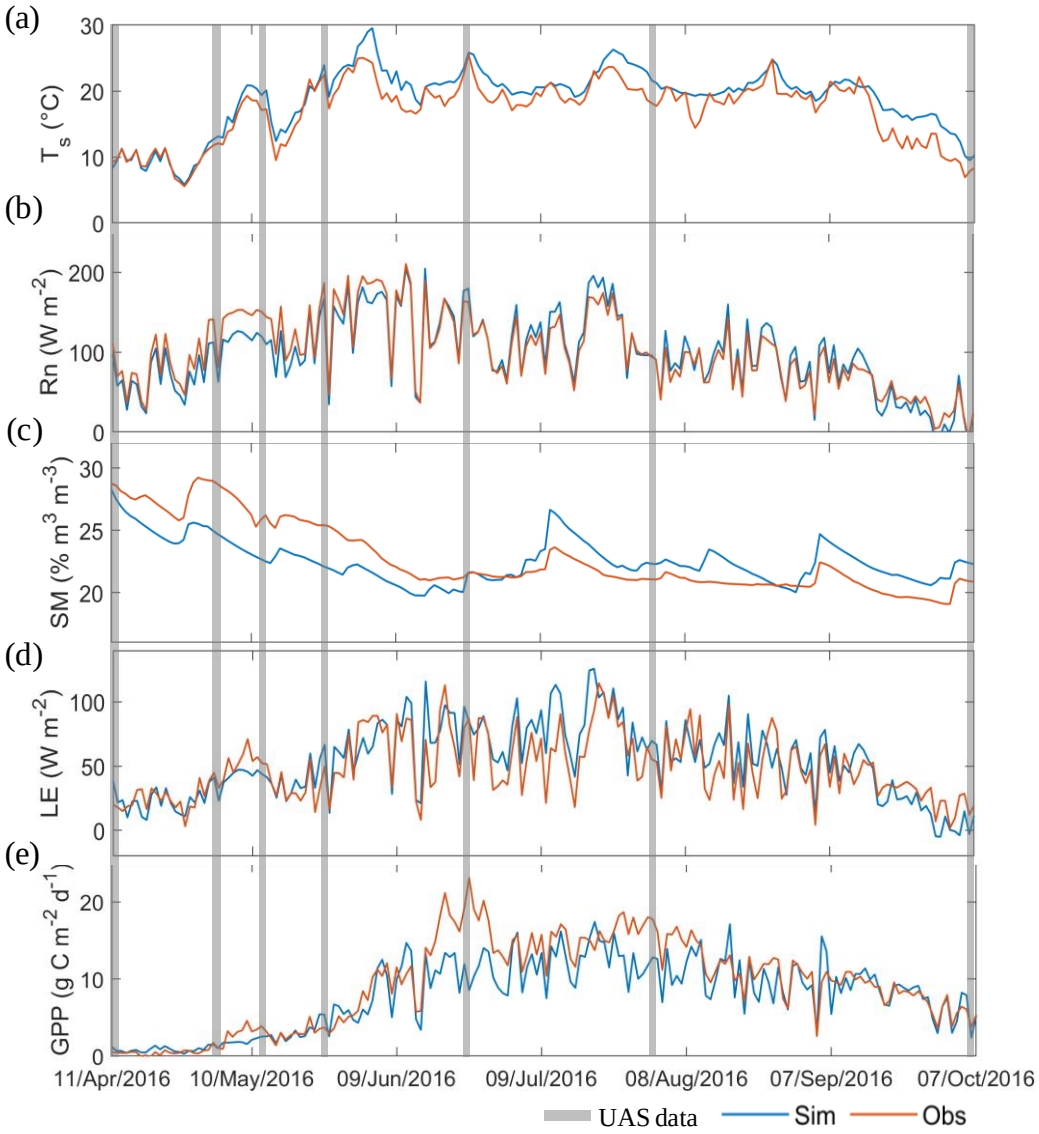

Figure 5~~6~~. Simulated continuous daily land surface variables from 11th April to 7th October 2016 in the willow plantation. (a) Land surface temperature T_s, (b) Net radiation Rn, (c) Soil moisture θ, (d) Latent heat flux LE, and (e) Gross primary productivity GPP. The dashed area indicates the time of acquired data for model calibration. The blue and red curves represent simulations and observations, respectively.

~~Figure 5 (c) shows that t~~The estimated ~~SM~~θ from ~~the~~ SVEN ~~model~~ achieved ~~a~~ moderate performance in terms of ~~error~~errors and correlation. The model underestimates ~~SM~~θ when NDVI is low, ~~and~~but overestimates ~~SM when NDVI is~~θ with high NDVI as ~~shown in~~ Figure ~~6~~ 7 (c). ~~This~~Such errors may be due to the uncertainty in the model parameters related to ~~SM and the error propagation from the remote sensing based SM~~θ. As shown in supplemental Table S5, the effective parameter

values of the infiltration rate for the saturated soil (Ks) and fitting parameter of the Mualem model (n) were taken as the mean values from the look-up table without considering ranges of variability (standard deviations in the table). In fact, only one parameter, SWS_{max}, among the three parameters related to ~~SM~~θ dynamics was calibrated with UAS estimates of ~~SM~~θ in the root zone. To keep the model simple, the SVEN model only used one soil layer to simulate the dynamics of soil water storage (Figure 3). Such simplification could also contribute to the relatively moderate performance of simulating θ. Additionally, ~~the SM~~UAS derived θ estimates used for calibration have ~~also~~ errors of around 13% compared to the direct measurements (Wang et al., 2018a~~) that~~), which can ~~propagate~~induce uncertainties in the simulated time series through error propagates in the parameter calibration. Furthermore, only seven snapshot estimates from UAS were used to calibrate the model with an average frequency of 25 days during the period of fast growth. It can be expected that improving the ~~better~~ UAS based ~~snapshot~~ estimates of ~~SM~~θ and increasing the number of observations for model calibration can improve the simulation performance.

The results of the simulated LE and GPP are shown in Figure ~~5~~ 6 (d) and (e), respectively. In most cases, ~~It can be seen that the~~ the simulation ~~overestimated~~ shows the overestimation of LE~~. This can be improved with better~~, which closely relates to the estimates of Rn and ~~SM~~θ. ~~From the scatterplot of Figure 5 (e), t~~The simulation underestimated GPP, as the parameter LUE_{max} was assumed to be the same as from a ~~nearly~~ nearby beech forest (Wang et al., 2018a). Even though both sites are temperate deciduous forests, ~~there is difference~~differences still exist between the natural beech forest and the willow forest bioenergy plantation. ~~It should be noted that~~Notably, there is a significant underestimation of the simulated GPP in June of 2016 as shown in Figure ~~5~~ 6 (e). Besides the possible uncertainties from the LUE_{max} described above, ~~this~~the underestimation may also result from the observation uncertainties in partitioning of GPP and respiration in ~~the~~ eddy covariance data processing~~ used in validation.~~. In~~ the~~ data processing, the night time net ecosystem exchanges were used to calculate the ecosystem respiration. During the night time, the eddy covariance footprint ~~has a large coverage~~extended well-beyond the edges of the willow forest of interest, due to the stable atmospheric conditions. The ~~ploughing activities~~tillage practices in the nearby ~~field released CO_2 to the atmosphere. This~~Rapeseed fields (Fig. 1) could contribute overestimation of daytime ecosystem respiration, and thus ~~also~~ leads to the overestimation of GPP in the eddy covariance data processing.

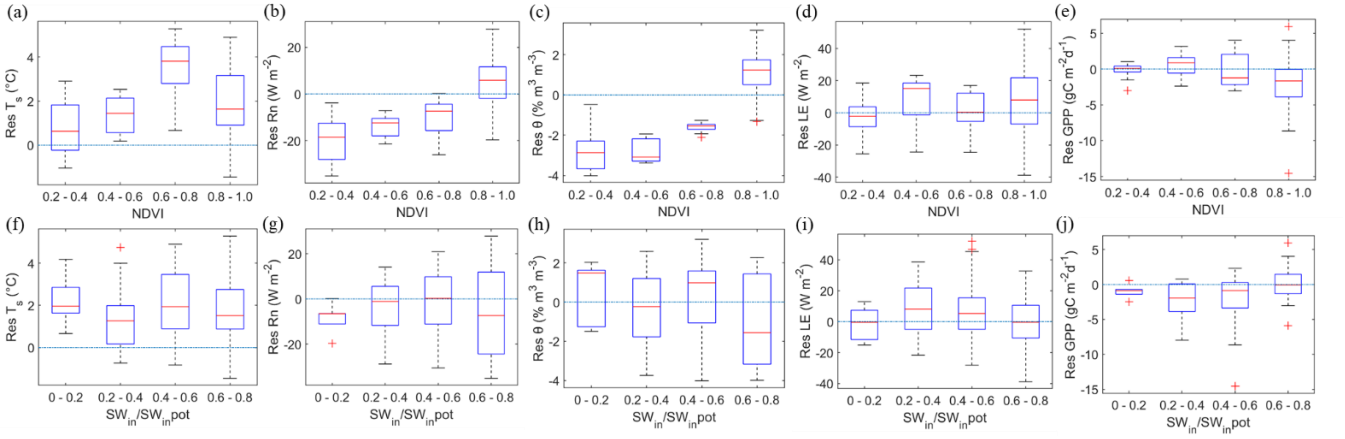

Figure 67. Boxplots of the residuals for the daily simulation. (a-e) are simulation residuals and NDVI. (f-j) are simulation residuals and the ratio of the actual (SW_{in}) and potential ($SW_{in}pot$) solar radiation, which is an indicator of the cloudiness condition. (a, f) surface temperature T_s, (b, g) net radiation Rn, (c, h) soil moisture θ, (d, i) latent heat flux LE, and (e, j) gross primary productivity GPP. The blue dashed lines refer to the zero residuals.

5

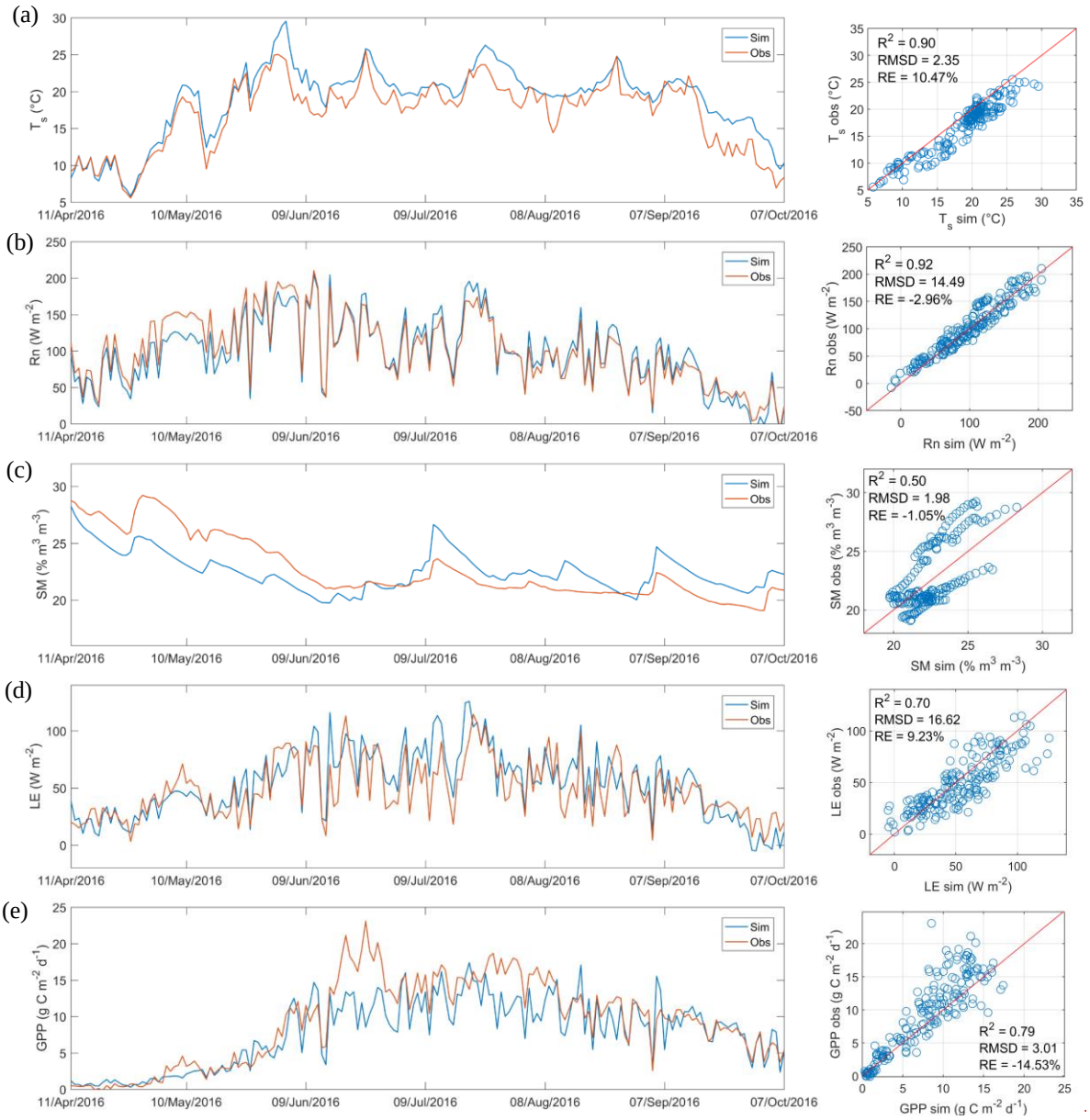

To check

the model simulation performance under cloudy~~**Figure 5.** Simulated continuous daily land surface variables from 11th April to 7th October 2016 in the willow plantation. (a) Land surface temperature T_s, (b) Net radiation Rn, (c) Soil moisture SM, (d) Latent heat flux LE, and (e) Gross primary productivity GPP.~~

conditions, we analysed the relationship between model residuals and the ratio representing the diffuse radiation fraction (Figure 7 f-j). There were no significant differences for the residuals of the simulated T_s, Rn, θ, LE and GPP under low and high diffuse radiation fraction conditions. Due to the ability of UAS to acquire data in both cloud cover and clear sky conditions, the SVEN model was capable of interpolating land surface variables under cloud cover conditions with similar skill as under clear sky conditions.

~~To check whether the model simulations are be good under overcast conditions, we analysed the relationship between model residuals and the ratio representing the diffuse radiation fraction and NDVI (Figure 6). Residuals of the simulated T_s, Rn, SM and LE do not show difference between low and high diffuse radiation fraction. The SVEN model was capable of interpolating LE and SM under cloud cover conditions with similar skill as under clear sky conditions but not GPP. GPP was underestimated under high diffuse radiation conditions and overestimated in the low diffuse radiation conditions. This is due to that the model did not consider the enhancement diffuse radiation effects on the plant carbon assimilation rate (Mercado et al., 2009; Roderick et al., 2001). It could be improved by incorporating an index representing the diffuse radiation fraction as Wang et al. (2018a), if higher accuracy is needed.~~

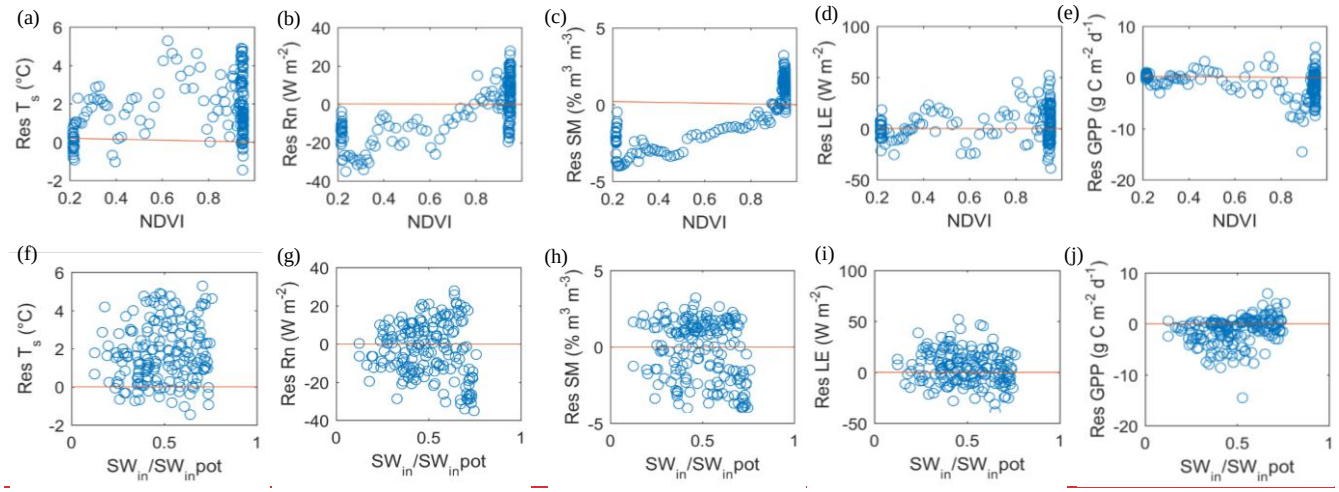

~~**Figure 6.** Model residuals for the daily simulation. (a-e) are relationship between model residuals and the ratio of the actual (SW_{in}) and potential (SW_{in}pot), which is an indicator for the diffuse radiation fraction. (f-j) are relationship between model residuals and NDVI. (a, f) surface temperature T_s, (b, g) net radiation Rn, (c, h) soil moisture SM, (d, i) latent heat flux LE, and (e, j) gross primary productivity GPP.~~

4.3 Validation at half-hourly and monthly time scales

Validation of the half-hourly and monthly T_s, Rn, ~~SM~~θ, LE and GPP by the SVEN model is shown in Figure ~~7~~8. The simulated half-hourly T_s, Rn, ~~SM~~θ, LE and GPP captured the temporal dynamics of land surface fluxes at this site. RMSDs for half-hourly T_s, Rn, ~~SM~~θ, LE and GPP are 3.04 °C, 63.82 W·m^{-2}, 1.99% m^3·m^{-3}, 56.37 W·m^{-2} and 6.14 μmol·C·m^{-2}·s^{-1}, respectively. ~~R^2 for T_s, Rn, SM, LE and GPP are 0.83, 0.89, 0.49, 0.78 and 0.77, respectively. At the monthly time scale, RMSDs for T_s, Rn, SM, LE and GPP are 2.10 °C, 10.96 W·m^{-2}, 1.86% m^3·m^{-3}, 9.09 W·m^{-2} and 1.82 g·C·m^{-2}·d^{-1}, respectively. R^2 for T_s, Rn, SM, LE and GPP are 0.96, 0.94, 0.61, 0.97 and 0.97, respectively. The metrics of RE for hourly and monthly scales are not shown, as they are the same as the RE at the daily scale.~~ Compared to the simulation performance at the daily time scale (as shown in Table 3), the half-hourly simulation has higher RMSDs and lower R^2. ~~However, the monthly simulation has better~~Such performance ~~than the~~ may be due to that parts of SVEN modules are more suitable for daily ~~with lower RMSDs and slightly higher R^2. When performing temporal averages, random errors cancel out. Additionally, the~~scale simulation instead of the half-hourly. For instance, the simulation of LE in SVEN ~~model~~ is based on the Priestley-Taylor equation originally applied to estimate monthly LE (Fisher et al., 2008) and was expended to be applied at daily steps (Garcia et al., 2013), but it is not appropriate for representing LE processes at sub-daily time scales.

Regarding the monthly time scale, RMSDs for T_s, Rn, θ, LE and GPP are 2.10 °C, 10.96 W·m^{-2}, 1.86% m^3·m^{-3}, 9.09 W·m^{-2} and 1.82 g·C·m^{-2}·d^{-1}, respectively. The monthly simulation has lower RMSDs and slightly higher R^2 compared to the daily simulation. The improvement of model performance from the half-hourly to daily and monthly time scales indicates the model errors can be reduced by aggregating the simulation outputs to longer time scales. ~~This~~Such accuracy also implies that the SVEN model has greater potential to temporally interpolate remote sensing observations at daily and monthly time scales, which are more relevant for applications in agriculture and ecosystem management.

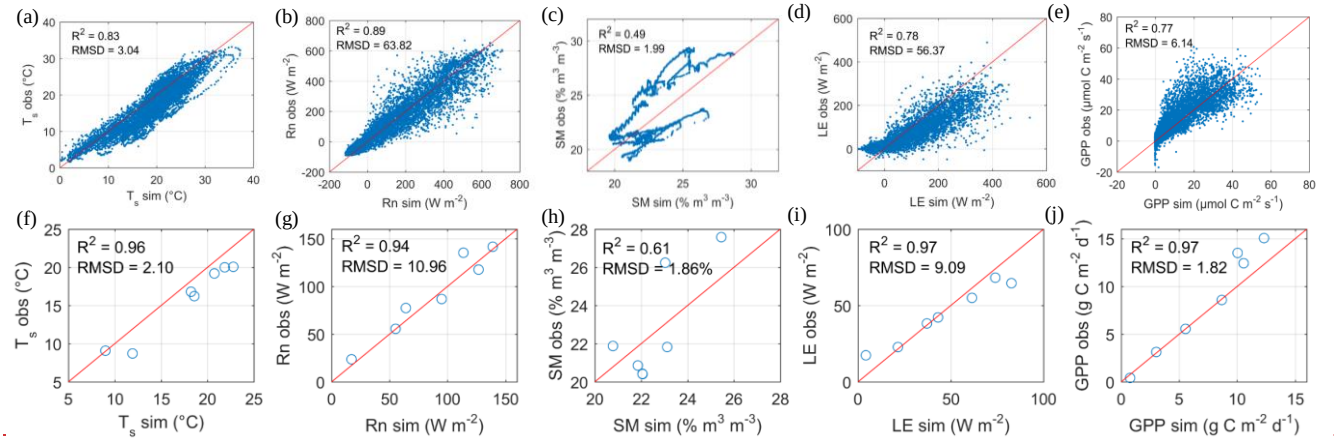

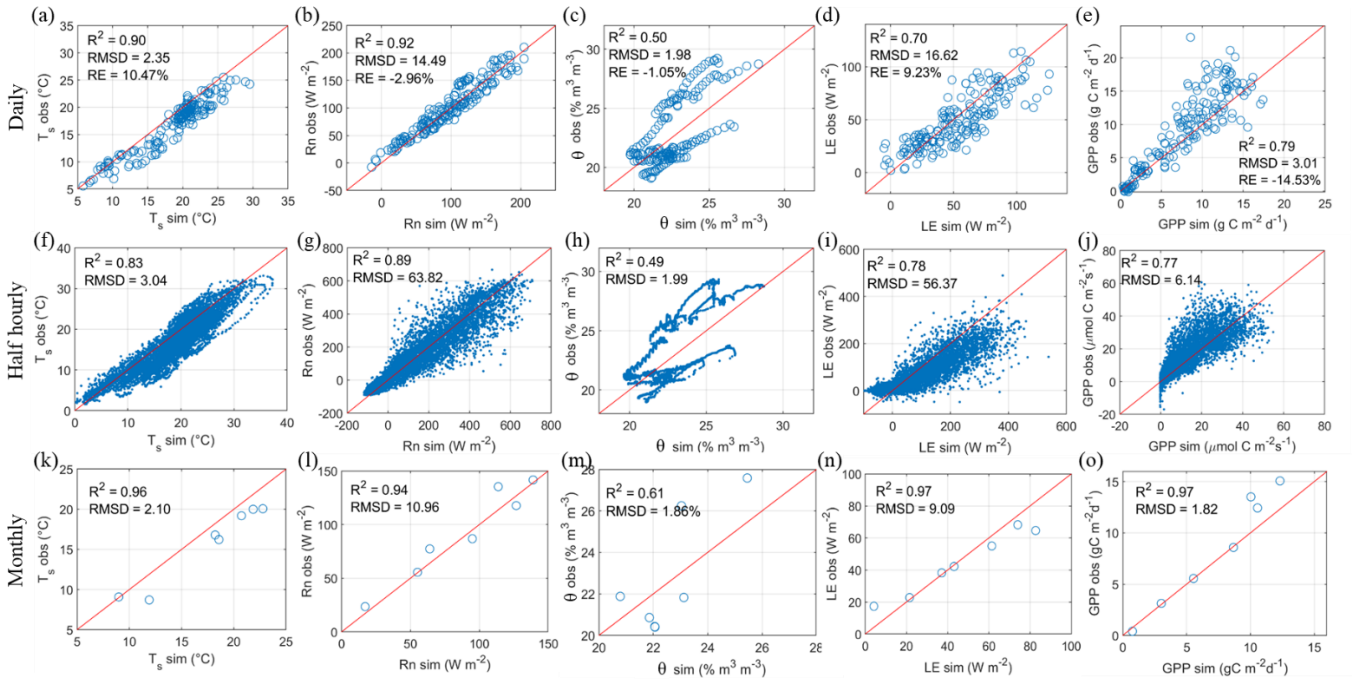

Figure ~~7~~8. Validation of the gap filled land surface variables at daily, half-hourly and monthly time scales in the willow plantation. (a-e) are at daily time scale, (f-j) are at half-~~-~~hourly time scale, and (~~f-j~~k-o) are at the monthly time scale. (a, f, k) land surface temperature T_s, (b, g, l) net radiation Rn, (c, h, m) soil moisture ~~SM~~θ, (d, ~~i~~I, m) latent heat flux LE, and (e, j, o) gross primary productivity GPP. The metrics of RE for hourly and monthly scales are not shown, as they are the same as the RE at the daily scale.

Table 3. Comparison of model simulation performance at half-~~-~~hourly, daily and monthly time scales.

Time scale	Statistics	Ts	Rn	~~SM~~θ	LE	GPP
Half hourly	R^2	0.83	0.89	0.49	0.78	0.77
	RMSD	3.04 °C	63.82 W·m^{-2}	1.99% m^3·m^{-3}	56.37 W·m^{-2}	6.14 μmol·C·m^{-2}·s^{-1}
	NRMSD	9.63%	8.41%	19.15%	10.49%	7.57%
Daily	R^2	0.9	0.92	0.5	0.7	0.79
	RMSD	2.35 °C	14.49 W·m^{-2}	1.98% m^3·m^{-3}	16.62 W·m^{-2}	3.01 g·C·m^{-2}·d^{-1}
	NRMSD	11.77%	6.65%	19.53%	14.77%	12.97%
Monthly	R^2	0.96	0.94	0.61	0.97	0.97
	RMSD	2.1 °C	10.96 W·m^{-2}	1.86% m^3·m^{-3}	9.09 W·m^{-2}	1.82 g·C·m^{-2}·d^{-1}
	NRMSD	18.49%	9.29%	25.91%	17.88%	12.42%

4.4 Potential applications and improvement of SVEN ~~model~~

This study showed that SVEN can be used as a tool to temporally interpolate land surface variables between remote sensing acquisitions with few meteorological data. In the statistical approaches, Alfieri et al. (2017) identified that a return interval of remote sensing observations should be no less than 5 days to accurately interpolate daily ET with relative errors less than 20%. The results shown from our model based interpolation approach ~~on~~ in a willow forest~~,~~ suggest~~s~~ that the revisit time for the remote sensing observations can potentially be extended. For instance, this study demonstrated that seven instantaneous observations/simulations with an averaged revisit time of 25 days can be used to accurately interpolate the daily ET for 180 days. This comparison shows the ~~great~~ benefits of using the model based approach to continuously estimate land surface fluxes from remote sensing based snapshot observations or ~~simulations~~estimates. The model based approach can be used to estimate ecosystem states and flux exchange with the atmosphere for a landscape (e.g. crop fields) with temporally sparse UAS flight campaigns. This approach has great potential for agricultural ecosystem monitoring and management. The interpolated continuous record of land surface variables can also further facilitate our understanding ~~on~~of the temporal dynamics of land surface-atmosphere flux exchanges.

On the other ~~hand~~side, this study also provides ideas to utilize remote sensing estimates or observations to improve land surface modeling. Traditionally, the applicability of land surface models is ~~restricted~~ limited due to complex model parameterization and the limited availability of "ground truth" or in-situ data for parameter calibration. As shown in this study, one solution for this limitation is ~~to~~ usinge remote sensing based ~~simulations~~ observations or estimates as "ground truth" for model calibration (Stisen et al., 2011; Zhang et al., 2009). This study calibrated the model parameters ~~using~~ through remote sensing snapshot (UAS) estimates of land surface variables such as T_s and ~~SM~~θ, and provided an example of integrating remote sensing data and process-based models. Other variables such as Rn, ET and GPP as shown in Figure 4 could also be incorporated for model calibration.

Compared to complex land surface models, this approach is simple and efficient~~. , It is~~ especially suitable for operational applications to interpolate the remote sensing based snapshot estimates into the temporally continuous values.

Both the look-up table and parameter optimization approaches were used in this study to obtain the parameter values. For instance, we used a look-up table (Carsel and Parrish, 1988) to get values of the fitting parameter of the Mualem model (n) and the infiltration rate for the saturated soil (K_s). The advantage of using the look-up table approach is that it can be easily applied according to the site conditions, such as vegetation types, soil texture and soil depth. However, this approach requires prior knowledge on the site. Insufficient knowledge of the site conditions may lead to the selection of unsuitable parameter values from the look-up tables. For instance, K_s may vary at different soil layers and it could be difficult to select an effective K_s to represent the condition for the entire soil layers. Regarding the optimization approach, this method has an advantage to achieve good fitting performance with UAS derived observations or estimates. However, this optimization approach needs to consider the number of observations and calibration parameters, parameter equifinality and multi-objective optimization (Her and Chaubey, 2015). For instance, due to limited fourteen UAS derived T_s or θ available for

calibration, we selected only four parameters (C_{sat}, b, C_{veg}, and SWS_{max}), which are hard to obtain from the look-up table approach with insufficient prior knowledge of the site, for optimization. To deal with parameter equifinality and multi-objective optimization, the Monte Carlo optimization was combined with the Pareto front analysis in this study. Other approaches e.g. Bayesian analysis could also be utilized to calibrate the model parameter with multiple objectives and separate the uncertainty sources: input, parameters and model structure (Vrugt et al., 2009). It can be a useful tool for the model calibration and quantification of the simulated uncertainty. Besides the look-up table and optimization approaches, another promising approach is to estimate soil or plant hydraulic properties from imaging spectroscopy (Goldshleger et al., 2012; Nocita et al., 2015) or thermal imaging data (Jones, 2004).

This model based interpolation approach can potentially also be applied with the space-borne remote sensing measurements to facilitate the temporally continuous estimation of large-scale land surface fluxes. The combination of the process-based models and satellite observations (e.g. Sentinel or MODIS land surface temperature and GPP products) can reduce the need of in-situ data for parameterizations. The temporally continuous estimates of land surface fluxes from satellite data facilitate our understanding of the temporal upscaling from instantaneous estimates to the daily or longer time scales to improve our knowledge of the coupled energy, water and carbon cycles at various temporal scales, particularly for data-scarcity regions. ~~The practicality of the proposed approach for describing surface fluxes and water budgets in sites without flux stations and direct field observations. It can be used to estimate ecosystem states and flux exchange with the atmosphere for a larger part of a landscape (e.g. farm) with temporally sparse UAS flight campaigns and online meteorological data. This has great potential to improve the management of agriculture ecosystems.~~ ~~for and forecasting~~However, there are also challenges and limitations for widespread applications of the proposed model to other regions or with satellite Earth observation. SVEN also requires further improvement to enhance its ability for large-scale applications. For instance, the current soil moisture module in SVEN model is a simple water balance model with considering one soil layer, which has limited capacity to simulate soil water dynamics particularly in regions with complex landforms. In addition, the soil layer depth refers to the maximum root water uptake depth, which can vary with time (Guderle and Hildebrandt, 2015), but SVEN simplified this soil depth parameter to keep it consistent. Thus, in our study, SVEN only achieved moderate performance to simulate soil water dynamics and it can be expected that in ~~dry~~water limited ~~controlled~~drylands, soil moisture simulation has a larger impact on the ET than in our site ~~regions this has a larger impact on the ET than in our site~~. Nonetheless, SVEN soil moisture estimates, relying on precipitation and water balance, should be in principle more accurate than those using thermal inertia (Garcia et al., 2013) , the original complementary approach relying on VPD (Fisher et al., 2008) or soil moisture proxies using antecedent precipitation proxies (Morillas et al., 2013; Zhang et al., 2010). Compared to the Penman-Monteith approach, the Priestley–Taylor approach may need adjustment of the aerodynamic term, when extending the study from radiation controlled sites to arid climates (Tadesse et al., 2018; Xiaoying and Erda, 2005). When applying SVEN to the large scale, the model needs to consider the sub-grid heterogeneity and identify the effective values for model parameters, e.g. soil saturated hydraulic conductance. The plant functional type and soil type parameterization scheme for different ecosystems and environmental conditions would be needed. Furthermore, there also remain challenges to get the reliability of

atmospheric forcing such as radiation, precipitation and wind speed. Accurate gridded meteorological data from reanalysis, remote sensing or weather forecasting models as forcing will be needed. Moreover, satellite based observations or estimates may have larger uncertainties due to the coarser spatial resolution than UAS estimates. Applying SVEN with satellite data to large scale, we also need to evaluate the accuracy of satellite products and consider the error propagation from remote sensing estimates to the simulation outputs. In addition, satellite data in the optical and thermal ranges can only provide observations during the cloudless conditions. The satellite data based model calibration may lead model estimates biased toward sunny weather conditions. ~~However, SVEN soil moisture estimates, relying on precipitation and water balance, should be in principle more accurate than those using thermal inertia (Garcia et al., 2013) , the original complementary approach relying on VPD (Fisher et al., 2008) or soil moisture proxies using antecedent precipitation proxies (Morillas et al., 2013; Zhang et al.,)~~

~~Both the look-up-table and parameter optimization approaches were used in this study to obtain the parameter values. For instance, we used a look-up-table (Carsel and Parrish, 1988) to get values of the fitting parameter of the Mualem model (n) and the infiltration rate for the saturated soil (K_s). The advantage of using the look-up-table approach is that it can be easily applied according to the site conditions, such as vegetation types, soil texture and soil depth. However, this approach requires prior knowledge on the site. Insufficient knowledge on the site conditions may lead to the selection of unsuitable parameter values from the look-up tables. For instance, K_s may vary at different soil layers and it could be difficult to select an effective K_s to represent the condition for the entire soil layers.~~

~~Regarding the optimization approach, this method has an advantage to achieve a good fitting performance with UAS observations or estimates. However, this optimization approach needs to consider the number of observations and calibration parameters, parameter equifinality and multi-objective optimization (Her and Chaubey, 2015). For instance, due to limited fourteen UAS T_s or SM available for calibration, we selected only four parameters (C_{sat}, b, C_{veg}, and SWS_{max}), which are hard to obtain from the look-up-table approach with insufficient prior knowledge of the site, for optimization. To deal with parameter equifinality and multi-objective optimization, the Monte Carlo optimization was combined with the Pareto front analysis in this study. Other approaches e.g. Bayesian analysis could also be utilized to calibrate the model parameter with multiple objectives and separate the uncertainty sources: input, parameters and model structure (Vrugt et al., 2009). It can be a useful tool for the model calibration and quantification of the simulated uncertainty. Besides the look-up-table and optimization approaches, another promising approach is to estimate soil or plant hydraulic properties from imaging spectroscopy (Goldshleger et al., 2012; Nocita et al., 2015) or thermal imaging data (Jones, 2004).~~

5 Conclusion

Continuous estimation of land surface variables, such as surface temperature, net radiation, soil moisture, evapotranspiration and gross primary productivity at daily or monthly time scales is important for hydrological and ecological applications. However, remotely sensed observations ~~can be~~were limited to directly ~~used to~~ estimate the instantaneous status of land

surface variables at the time of data acquisitions. Therefore, to continuously estimate land surface variables from remote sensing, this study developed a tool to fill the temporal gaps of land surface fluxes between data acquisitions and interpolate instantaneous estimates into continuous records. The tool is a dynamic Soil Vegetation Atmosphere Transfer model, the Soil-Vegetation, Energy, water and CO_2 traNsfer model (SVEN), which is a parsimonious model to continuously simulate land surface variables with meteorological forcing and vegetation indices as model forcing. To interpolate the snapshot estimates from UAS, this study conducted the model parameter calibration to integrate the SVEN model and the snapshot estimates of surface temperature and soil moisture at the time of flight. ~~This~~Such model-data integration provides an effective way to continuously estimate land surface fluxes from remotely sensed observations. A case study was conducted with seven temporally sparse observations from UAS multispectral and thermal sensors in a Danish willow bioenergy plantation (DK-RCW) during the growing season of 2016 (180 days). Satisfactory results were achieved with the root mean square deviations for the simulated daily land surface temperature, net radiation, soil moisture, latent heat flux and gross primary productivity equal to 2.35 °C, 14.49 $W \cdot m^{-2}$, 1.98% $m^3 \cdot m^{-3}$, 16.62 $W \cdot m^{-2}$ and 3.01 $g \cdot C \cdot m^{-2} \cdot d^{-1}$, respectively.

This model based interpolation method has potential not just with UAS but also with remotely sensed data from other platforms, e.g. satellite and manned airborne systems, for a range of spatial and temporal scales. ~~similar to more complex existing . While LSM would require information about for parameterization, the possibility to calibrate several model parameters using ET or soil moisture estimates from satellite sensors, as done in this study with UAS, reducing the need of in situ data for parameterizations. KALMAN FILTER ? However, uncertainties related with Additionally, the combination of the model based interpolation approach and remotely sensed observations (e.g. Sentinel or MODIS land surface temperature and GPP products) can facilitate our understanding on the temporal upscaling of instantaneous estimates to the daily or longer time scales to improve our knowledge of the coupled energy, water and carbon cycles at various temporal scales.~~

Data and code availability. The data and code used in this study are available upon request from the corresponding authors.

Supplement. The supplement related to this article is available online.

Author contribution. All authors contributed to the design of this study and model development. MG and PBG contributed to funding acquisition. AI made contributions to the eddy covariance and meteorological data. SW conducted model simulations and UAV data collection. SW wrote the original draft. All authors contributed to the discussion of the results and the revision of this paper.

Competing interests. The authors declare that they have no conflict of interest.

Acknowledgement: The authors would like to thank the EU and Innovation Fund Denmark (IFD) for funding, in the frame of the collaborative international consortium AgWIT financed under the ERA-NET Co-fund Water Works 2015 Call. This

ERA-NET is an integral part of the 2016 Joint Activities developed by the Water Challenges for a Changing World Joint Programme Initiative (Water JPI). This study was also supported by the Smart UAV project from IFD [125-2013-5]. SW was financed from an internal PhD grant from the Department of Environmental Engineering at DTU and was financed by the COST action OPTIMISE for a short-term research stage.

References

Alfieri, J. G., Anderson, M. C., Kustas, W. P. and Cammalleri, C.: Effect of the revisit interval and temporal upscaling methods on the accuracy of remotely sensed evapotranspiration estimates, Hydrol. Earth Syst. Sci., 21(1), 83–98, doi:10.5194/hess-21-83-2017, 2017.

Berni, J., Zarco-Tejada, P. J., Suarez, L. and Fereres, E.: Thermal and Narrowband Multispectral Remote Sensing for Vegetation Monitoring From an Unmanned Aerial Vehicle, IEEE Trans. Geosci. Remote Sens., 47(3), 722–738, doi:10.1109/TGRS.2008.2010457, 2009.

Boegh, E., Poulsen, R. N., Butts, M., Abrahamsen, P., Dellwik, E., Hansen, S., Hasager, C. B., Ibrom, A., Loerup, J. K., Pilegaard, K. and Soegaard, H.: Remote sensing based evapotranspiration and runoff modeling of agricultural, forest and urban flux sites in Denmark: From field to macro-scale, J. Hydrol., 377(3–4), 300–316, doi:10.1016/j.jhydrol.2009.08.029, 2009.

Brutsaert, W.: Evaporation into the Atmosphere. Theory, History, and Applications; Dordrecht: Holland, D, Reidel Co, 1982.

Calvet, J.-C., Noilhan, J. and Bessemoulin, P.: Retrieving the Root-Zone Soil Moisture from Surface Soil Moisture or Temperature Estimates: A Feasibility Study Based on Field Measurements, J. Appl. Meteorol., doi:10.1175/1520-0450(1998)037<0371:RTRZSM>2.0.CO;2, 1998.

Carlson, T. N., Gillies, R. R. and Schmugge, T. J.: An interpretation of methodologies for indirect measurement of soil water content, Agric. For. Meteorol., 77(3–4), 191–205, doi:10.1016/0168-1923(95)02261-U, 1995.

Carsel, R. F. and Parrish, R. S.: Developing joint probability distributions of soil water retention characteristics, Water Resour. Res., 24(5), 755–769, doi:10.1029/WR024i005p00755, 1988.

Catmull, E. and Rom, R.: A CLASS OF LOCAL INTERPOLATING SPLINES, in Computer Aided Geometric Design., 1974.

Chen, Y., Xia, J., Liang, S., Feng, J., Fisher, J. B., Li, X., Li, X., Liu, S., Ma, Z., Miyata, A., Mu, Q., Sun, L., Tang, J., Wang, K., Wen, J., Xue, Y., Yu, G., Zha, T., Zhang, L., Zhang, Q., Zhao, T., Zhao, L. and Yuan, W.: Comparison of satellite-based evapotranspiration models over terrestrial ecosystems in China, Remote Sens. Environ., 140, 279–293, doi:10.1016/j.rse.2013.08.045, 2014.

Choudhury, B. J. and Monteith, J. L.: A four-layer model for the heat budget of homogeneous land surfaces, Q. J. R. Meteorol. Soc., 114(480), 373–398, doi:10.1002/qj.49711448006, 1988.

Denis, G., Claverie, A., Pasco, X., Darnis, J. P., de Maupeou, B., Lafaye, M. and Morel, E.: Towards disruptions in Earth observation? New Earth Observation systems and markets evolution: Possible scenarios and impacts, Acta Astronaut., 137, 415–433, doi:10.1016/j.actaastro.2017.04.034, 2017.

Dettmann, U., Bechtold, M., Frahm, E. and Tiemeyer, B.: On the applicability of unimodal and bimodal van Genuchten-Mualem based models to peat and other organic soils under evaporation conditions, J. Hydrol., 515, 103–115, doi:10.1016/j.jhydrol.2014.04.047, 2014.

Djamai, N., Magagi, R., Goïta, K., Merlin, O., Kerr, Y. and Roy, A.: A combination of DISPATCH downscaling algorithm with CLASS land surface scheme for soil moisture estimation at fine scale during cloudy days, Remote Sens. Environ., 184, 1–14, doi:10.1016/j.rse.2016.06.010, 2016.

Ershadi, A., McCabe, M. F., Evans, J. P., Chaney, N. W. and Wood, E. F.: Multi-site evaluation of terrestrial evaporation models using FLUXNET data, Agric. For. Meteorol., 187, 46–61, doi:10.1016/j.agrformet.2013.11.008, 2014.

Fisher, J. B., Tu, K. P. and Baldocchi, D. D.: Global estimates of the land-atmosphere water flux based on monthly AVHRR and ISLSCP-II data, validated at 16 FLUXNET sites, Remote Sens. Environ., 112(3), 901–919, doi:10.1016/j.rse.2007.06.025, 2008.

Fisher, J. B., Melton, F., Middleton, E., Hain, C., Anderson, M., Allen, R., McCabe, M. F., Hook, S., Baldocchi, D., Townsend, P. A., Kilic, A., Tu, K., Miralles, D. D., Perret, J., Lagouarde, J. P., Waliser, D., Purdy, A. J., French, A., Schimel, D., Famiglietti, J. S., Stephens, G. and Wood, E. F.: The future of evapotranspiration: Global requirements for ecosystem functioning, carbon and climate feedbacks, agricultural management, and water resources, Water Resour. Res., 53(4), 2618–2626, doi:10.1002/2016WR020175, 2017.

Fratini, G., Ibrom, A., Arriga, N., Burba, G. and Papale, D.: Relative humidity effects on water vapour fluxes measured with closed-path eddy-covariance systems with short sampling lines, Agric. For. Meteorol., 165, 53–63, doi:10.1016/j.agrformet.2012.05.018, 2012.

GAO, W.: Parameterization Of Subgrid-Scale Land-Surface Fluxes With Emphasis On Distributing Mean Atmospheric Forcing And Using Satellite-Derived Vegetation Index, J. Geophys. Res., 100(D7), 14305–14317, doi:Doi 10.1029/95jd01464, 1995.

García, M., Sandholt, I., Ceccato, P., Ridler, M., Mougin, E., Kergoat, L., Morillas, L., Timouk, F., Fensholt, R. and Domingo, F.: Actual evapotranspiration in drylands derived from in-situ and satellite data: Assessing biophysical constraints, Remote Sens. Environ., 131, 103–118, doi:10.1016/j.rse.2012.12.016, 2013.

Garratt, J. R. and Hicks, B. B.: Momentum, heat and water vapour transfer to and from natural and artificial surfaces, Q. J. R. Meteorol. Soc., 99(422), 680–687, doi:10.1002/qj.49709942209, 1973.

Goldshleger, N., Chudnovsky, A. and Ben-Dor, E.: Using reflectance spectroscopy and artificial neural network to assess water infiltration rate into the soil profile, Appl. Environ. Soil Sci., doi:10.1155/2012/439567, 2012.

Van de Griend and M.Owe., A. A.: On the relationship between thermal emissivity\nand normalized vegetation index for natural surfaces, Int. J. Remote Sens., 14(6), 1119–1131, doi:10.1080/01431169308904400, 1993.

Guderle, M. and Hildebrandt, A.: Using measured soil water contents to estimate evapotranspiration and root water uptake profiles-a comparative study, Hydrol. Earth Syst. Sci., doi:10.5194/hess-19-409-2015, 2015.

Her, Y. and Chaubey, I.: Impact of the numbers of observations and calibration parameters on equifinality, model performance, and output and parameter uncertainty, Hydrol. Process., doi:10.1002/hyp.10487, 2015.

Huang, F., Zhan, W., Duan, S. B., Ju, W. and Quan, J.: A generic framework for modeling diurnal land surface temperatures with remotely sensed thermal observations under clear sky, Remote Sens. Environ., 150, 140–151, doi:10.1016/j.rse.2014.04.022, 2014.

Huang, F., Zhan, W., Voogt, J., Hu, L., Wang, Z., Quan, J., Ju, W. and Guo, Z.: Temporal upscaling of surface urban heat island by incorporating an annual temperature cycle model: A tale of two cities, Remote Sens. Environ., 186, 1–12, doi:10.1016/j.rse.2016.08.009, 2016.

Huning, L. S. and Margulis, S. A.: Watershed modeling applications with a modular physically-based and spatially-distributed watershed educational toolbox, Environ. Model. Softw., doi:10.1016/j.envsoft.2015.02.008, 2015.

Ibrom, A., Dellwik, E., Flyvbjerg, H., Jensen, N. O. and Pilegaard, K.: Strong low-pass filtering effects on water vapour flux measurements with closed-path eddy correlation systems, Agric. For. Meteorol., 147(3–4), 140–156, doi:10.1016/j.agrformet.2007.07.007, 2007.

Jin, Y., Ge, Y., Wang, J. and Heuvelink, G. B. M.: Deriving temporally continuous soil moisture estimations at fine resolution by downscaling remotely sensed product, Int. J. Appl. Earth Obs. Geoinf., 68, 8–19, doi:10.1016/j.jag.2018.01.010, 2018.

Jones, H. G.: Application of Thermal Imaging and Infrared Sensing in Plant Physiology and Ecophysiology., 2004.

Jung, M., Reichstein, M., Margolis, H. A., Cescatti, A., Richardson, A. D., Arain, M. A., Arneth, A., Bernhofer, C., Bonal, D., Chen, J., Gianelle, D., Gobron, N., Kiely, G., Kutsch, W., Lasslop, G., Law, B. E., Lindroth, A., Merbold, L., Montagnani, L., Moors, E. J., Papale, D., Sottocornola, M., Vaccari, F. and Williams, C.: Global patterns of land-atmosphere fluxes of carbon dioxide, latent heat, and sensible heat derived from eddy covariance, satellite, and meteorological observations, J. Geophys. Res. Biogeosciences, 116(3), doi:10.1029/2010JG001566, 2011.

Malbéteau, Y., Merlin, O., Balsamo, G., Er-Raki, S., Khabba, S., Walker, J. P. and Jarlan, L.: Toward a Surface Soil Moisture Product at High Spatiotemporal Resolution: Temporally Interpolated, Spatially Disaggregated SMOS Data, J. Hydrometeorol., 19(1), 183–200, doi:10.1175/JHM-D-16-0280.1, 2018.

McCabe, M. F., Rodell, M., Alsdorf, D. E., Miralles, D. G., Uijlenhoet, R., Wagner, W., Lucieer, A., Houborg, R., Verhoest, N. E. C., Franz, T. E., Shi, J., Gao, H. and Wood, E. F.: The future of Earth observation in hydrology, Hydrol. Earth Syst. Sci., 21(7), 3879–3914, doi:10.5194/hess-21-3879-2017, 2017.

McCallum, I., Wagner, W., Schmullius, C., Shvidenko, A., Obersteiner, M., Fritz, S. and Nilsson, S.: Satellite-based terrestrial production efficiency modeling., Carbon Balance Manag., 4(1), 8, doi:10.1186/1750-0680-4-8, 2009.

Miralles, D. G., Jiménez, C., Jung, M., Michel, D., Ershadi, A., Mccabe, M. F., Hirschi, M., Martens, B., Dolman, A. J., Fisher, J. B., Mu, Q., Seneviratne, S. I., Wood, E. F. and Fernández-Prieto, D.: The WACMOS-ET project - Part 2:

Evaluation of global terrestrial evaporation data sets, Hydrol. Earth Syst. Sci., 20(2), 823–842, doi:10.5194/hess-20-823-2016, 2016.

Monteith, J. L.: Solar Radiation and Productivity in Tropical Ecosystems, J. Appl. Ecol., 9(3), 747, doi:10.2307/2401901, 1972.

Mu, Q., Zhao, M. and Running, S. W.: MODIS Global Terrestrial Evapotranspiration (ET) Product (MOD16A2/A3) - ATBD Collection 5, , 66, 2013.

Mualem, Y.: New Model for Predicting Hydraulic Conductivity of Unsaturated Porous-Media, Water Resour. Res., 12(3), 513–522, doi:Doi 10.1029/Wr012i003p00513, 1976.

Nocita, M., Stevens, A., van Wesemael, B., Aitkenhead, M., Bachmann, M., Barthes, B., Dor, E. B., Brown, D. J., Clairotte, M., Csorba, A., Dardenne, P., DemattÃa, J. A., Genot, V., Guerrero, C., Knadel, M., Montanarella, L., Noon, C., Ramirez-Lopez, L. and Wetterlind, J.: Chapter Four - Soil Spectroscopy: An Alternative to Wet Chemistry for Soil Monitoring, Adv. Agron., 2015.

Noilhan, J. and Mahfouf, J. F.: The ISBA land surface parameterisation scheme, Glob. Planet. Change, 13(1–4), 145–159, doi:10.1016/0921-8181(95)00043-7, 1996.

Noilhan, J. and Planton, S.: A Simple Parameterization of Land Surface Processes for Meteorological Models, Mon. Weather Rev., 117(3), 536–549, doi:10.1175/1520-0493(1989)117<0536:ASPOLS>2.0.CO;2, 1989.

Pilegaard, K., Ibrom, A., Courtney, M. S., Hummelshøj, P. and Jensen, N. O.: Increasing net CO2 uptake by a Danish beech forest during the period from 1996 to 2009, Agric. For. Meteorol., 151(7), 934–946, doi:10.1016/j.agrformet.2011.02.013, 2011.

Potter, C. S., Randerson, J. T., Field, C. B., Matson, P. A., Vitousek, P. M., Mooney, H. A. and Klooster, S. A.: Terrestrial ecosystem production: A process model based on global satellite and surface data, Global Biogeochem. Cycles, 7(4), 811–841, doi:10.1029/93GB02725, 1993.

Priestley, C. and Taylor, R.: On the assessment of surface heat flux and evaporation using large-scale parameters, Mon. Weather Rev., (February), 81–92, doi:10.1175/1520-0493(1972)100<0081:OTAOSH>2.3.CO;2, 1972.

Reichstein, M., Falge, E., Baldocchi, D., Papale, D., Aubinet, M., Berbigier, P., Bernhofer, C., Buchmann, N., Gilmanov, T., Granier, A., Grünwald, T., Havránková, K., Ilvesniemi, H., Janous, D., Knohl, A., Laurila, T., Lohila, A., Loustau, D., Matteucci, G., Meyers, T., Miglietta, F., Ourcival, J. M., Pumpanen, J., Rambal, S., Rotenberg, E., Sanz, M., Tenhunen, J., Seufert, G., Vaccari, F., Vesala, T., Yakir, D. and Valentini, R.: On the separation of net ecosystem exchange into assimilation and ecosystem respiration: Review and improved algorithm, Glob. Chang. Biol., 11(9), 1424–1439, doi:10.1111/j.1365-2486.2005.001002.x, 2005.

Running, S. W. and Coughlan, J. C.: A general model of forest ecosystem processes for regional applications I. Hydrologic balance, canopy gas exchange and primary production processes, Ecol. Modell., 42(2), 125–154, doi:10.1016/0304-3800(88)90112-3, 1988.

Running, S. W., Nemani, R. R., Heinsch, F. A. N. N., Zhao, M., Reeves, M. and Hashimoto, H.: A Continuous Satelite-

lDerived Measure of Global Terrestrial Primary Production, Bioscience, 54(6), 547, doi:10.1641/0006-3568(2004)054, 2004.

Sandholt, I., Rasmussen, K. and Andersen, J.: A simple interpretation of the surface temperature/vegetation index space for assessment of surface moisture status, Remote Sens. Environ., 79(2–3), 213–224, doi:10.1016/S0034-4257(01)00274-7, 2002.

Sellers, P. J., Randall, D. A., Collatz, G. J., Berry, J. A., Field, C. B., Dazlich, D. A., Zhang, C., Collelo, G. D. and Bounoua, L.: A revised land surface parameterization (SiB2) for atmospheric GCMs. Part I: Model formulation, J. Clim., 9(4), 676–705, doi:10.1175/1520-0442(1996)009<0676:ARLSPF>2.0.CO;2, 1996.

Shuttleworth, W. J. and Wallace, J. S.: Evaporation from sparse crops-an energy combination theory, Q. J. R. Meteorol. Soc., 111(465), 839–855, doi:10.1002/qj.49711146510, 1985.

Stisen, S., McCabe, M. F., Refsgaard, J. C., Lerer, S. and Butts, M. B.: Model parameter analysis using remotely sensed pattern information in a multi-constraint framework, J. Hydrol., doi:10.1016/j.jhydrol.2011.08.030, 2011.

Tadesse, H. K., Moriasi, D. N., Gowda, P. H., Marek, G., Steiner, J. L., Brauer, D., Talebizadeh, M., Nelson, A. and Starks, P.: Evaluating evapotranspiration estimation methods in APEX model for dryland cropping systems in a semi-arid region, Agric. Water Manag., doi:10.1016/j.agwat.2018.04.007, 2018.

Twine, T. E., Kustas, W. P., Norman, J. M., Cook, D. R., Houser, P. R., Meyers, T. P., Prueger, J. H., Starks, P. J. and Wesely, M. L.: Correcting eddy-covariance flux underestimates over a grassland, Agric. For. Meteorol., 103(3), 279–300, doi:10.1016/S0168-1923(00)00123-4, 2000.

Vinukollu, R. K., Meynadier, R., Sheffield, J. and Wood, E. F.: Multi-model, multi-sensor estimates of global evapotranspiration: climatology, uncertainties and trends, Hydrol. Process., 25(26), 3993–4010, doi:10.1002/hyp.8393, 2011.

Vrugt, J. A., ter Braak, C. J. F., Gupta, H. V. and Robinson, B. A.: Equifinality of formal (DREAM) and informal (GLUE) Bayesian approaches in hydrologic modeling?, Stoch. Environ. Res. Risk Assess., doi:10.1007/s00477-008-0274-y, 2009.

Wang, S., Ibrom, A., Bauer-Gottwein, P. and Garcia, M.: Incorporating diffuse radiation into a light use efficiency and evapotranspiration model: An 11-year study in a high latitude deciduous forest, Agric. For. Meteorol., 248(July), 479–493, doi:10.1016/j.agrformet.2017.10.023, 2018a.

Wang, S., Garcia, M., Ibrom, A., Jakobsen, J., Josef Köppl, C., Mallick, K., Looms, M. and Bauer-Gottwein, P.: Mapping Root-Zone Soil Moisture Using a Temperature–Vegetation Triangle Approach with an Unmanned Aerial System: Incorporating Surface Roughness from Structure from Motion, Remote Sens., 10(12), 1978, 2018b.

Wang, S., Garcia, M., Bauer-Gottwein, P., Jakobsen, J., Zarco-Tejada, P. J., Bandini, F., Paz, V. S. and Ibrom, A.: High spatial resolution monitoring land surface energy, water and CO 2 fluxes from an Unmanned Aerial System, Remote Sens. Environ., doi:10.1016/j.rse.2019.03.040, 2019a.

Wang, S., Baum, A., Zarco-Tejada, P. J., Dam-Hansen, C., Thorseth, A., Bauer-Gottwein, P., Bandini, F. and Garcia, M.: Unmanned Aerial System multispectral mapping for low and variable solar irradiance conditions: Potential of tensor decomposition, ISPRS J. Photogramm. Remote Sens., 155(June), 58–71, doi:10.1016/j.isprsjprs.2019.06.017, 2019b.

Westermann, S., Langer, M. and Boike, J.: Spatial and temporal variations of summer surface temperatures of high-arctic

tundra on Svalbard - Implications for MODIS LST based permafrost monitoring, Remote Sens. Environ., 115(3), 908–922, doi:10.1016/j.rse.2010.11.018, 2011.

Wilson, K., Goldstein, A., Falge, E., Aubinet, M., Baldocchi, D., Berbigier, P., Bernhofer, C., Ceulemans, R., Dolman, H., Field, C., Grelle, A., Ibrom, A., Law, B. E., Kowalski, A., Meyers, T., Moncrieff, J., Monson, R., Oechel, W., Tenhunen, J., Valentini, R. and Verma, S.: Energy balance closure at FLUXNET sites, Agric. For. Meteorol., 113(1–4), 223–243, doi:10.1016/S0168-1923(02)00109-0, 2002.

Wutzler, T., Lucas-Moffat, A., Migliavacca, M., Knauer, J., Sickel, K., Šigut, L., Menzer, O. and Reichstein, M.: Basic and extensible post-processing of eddy covariance flux data with REddyProc, Biogeosciences, 15(16), 5015–5030, doi:10.5194/bg-15-5015-2018, 2018.

Xiaoying, L. and Erda, L.: Performance of the Priestley-Taylor equation in the semiarid climate of North China, Agric. Water Manag., doi:10.1016/j.agwat.2004.07.007, 2005.

Yapo, P. O., Gupta, H. V. and Sorooshian, S.: Multi-objective global optimization for hydrologic models, J. Hydrol., doi:10.1016/S0022-1694(97)00107-8, 1998.

Zhang, X., Pang, J. and Li, L.: Estimation of Land Surface temperature under cloudy skies using combined diurnal solar radiation and surface temperature evolution, Remote Sens., 7(1), 905–921, doi:10.3390/rs70100905, 2015.

Zhang, Y., Chiew, F. H. S., Zhang, L. and Li, H.: Use of remotely sensed actual evapotranspiration to improve rainfall-runoff modeling in Southeast Australia, J. Hydrometeorol., doi:10.1175/2009JHM1061.1, 2009.